



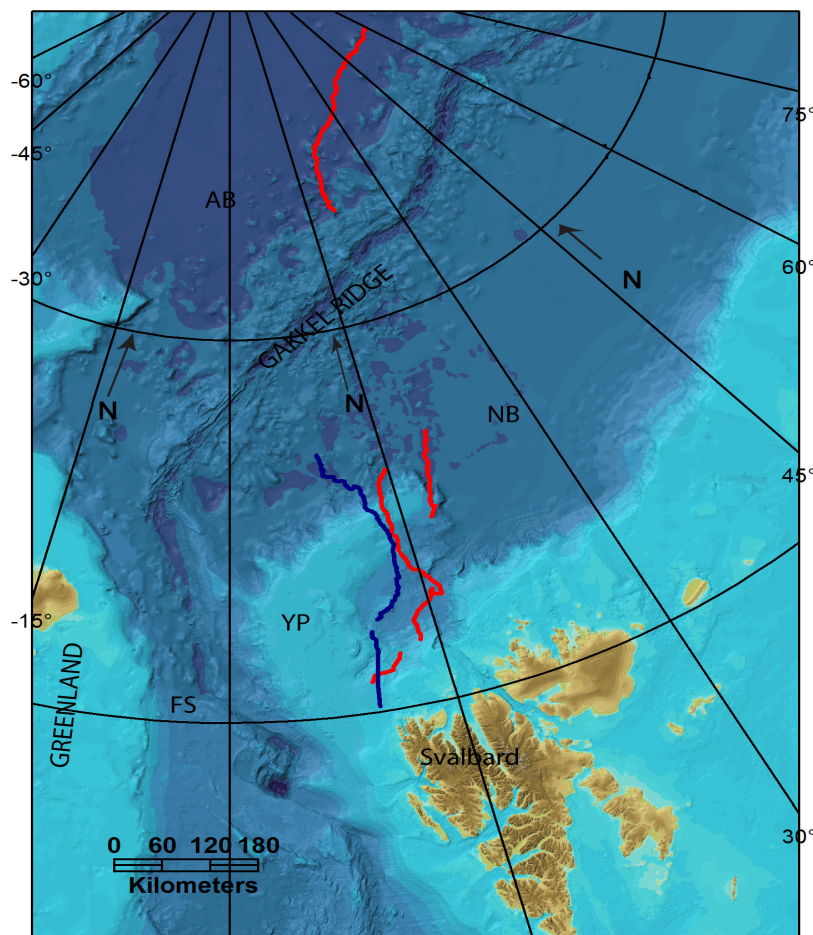
Stockholm
University

Master Thesis

Degree Project in
Marine Geology 60 hp

Acoustic stratigraphy and evidence of submarine landforms over the Yermak Plateau

Hamad Ali



Stockholm 2014

Department of Geological Sciences
Stockholm University
SE-106 91 Stockholm

Saying of the Al-Quran

“Observe what is in the heaven and the earth “But of no avail will be signs or warners to people who do not believe.”

Surah Younas Ayat No. 101

Saying of the Holy Prophet (Peace Be Upon Him)

“Do you know who is the most beneficent, God is the most beneficent, then the children of the man; I am the most beneficent and after me, the most beneficent among them is the man who acquires knowledge and spreads it, he will come on the day of resurrection as a chief by himself.”

Dedicated To

Hazrat Muhammad (PBUH)

Who guides us towards the path of success.

My Loving Mother and Caring (late) Father

*Who determined the path and destination for me and who always make things possible
for me.*

My Wife, Brothers and Sisters

Whose prays and support enabled me to complete my studies.

ACKNOWLEDGEMENT

All the praises and thanks to the gracious and the greatest Almighty ALLAH, the Lord of mankind and all that exists. Lots of blessings to the Holy Prophet Hazrat Muhammad (SAW) who is the real source of wisdom, guidance and knowledge for the whole humanity.

I feel highly privileged in taking opportunity to express my deepest gratitude and sincerest thanks to my respected project supervisors Richard Gyllencreutz and Martin Jakobsson department of geological sciences, Stockholm University , for their kind supervision, proper guidance, valuable and expert suggestions and great enthusiasm throughout the research work.

I offer my heartiest thanks to Tom Floden for their affectionate attitude, constant help and advices, and special gratitude to honorable Eve Arnold for her cooperation and sincerest support during my project and master's studies.

I would also like to express my deepest thanks to all University staff and my friends Anita, Francis, Martina, Oscar, Farhan and Roohullah whose advices and sincere cooperation encourages me during my master's studies and this project.

I would like to thanks the AGAVE 2007 and LOMROG II 2009 expedition's captain and crew to collect the data for making this study possible.

May Allah bless all these people with all of His blessings (Aamin).

Abstract

New high-resolution geophysical evidence on the seafloor morphology and acoustic stratigraphy of the Yermak Plateau and northern Svalbard margin between 80° and 83° 50 N, 5° and 22° E is presented in this study. Geophysical datasets are derived from swath bathymetry and sub-bottom acoustic profiling and correlated with nearby existing cores to derive chronological control. Seafloor landforms in the form of paleo iceberg ploughmarks of different dimensions, a paleo slump deposit and an erosional unconformity, all covered by subsequent sedimentation, are found. The erosional unconformity is overlain by an acoustically chaotic layer of about 15 m thickness. An abrupt change in acoustic stratigraphy in a small area (6 km long) on the southern YP resulting lower sedimentation rates is caused by the West Spitsbergen Current or a reverse southward bottom current flowing at the eastern Yermak Plateau slope.

The explanation for the iceberg ploughmarks on the southern Yermak Plateau is the flow of a major grounding ice sheet with several deep keeled ice originated from Svalbard shelf. The erosional unconformity could be caused by; (i) mass wasting, (ii) grounded ice sheet (iii) current controlled erosion. The reason for slumping is probably slope failure.

Keywords:

Fram Strait; Mass wasting; Yermak Plateau; Ploughmarks; Slump scars; West Spitsbergen Current; Marine geosciences; geophysics; sub-bottom profiling; multibeam echosounder.

Contents

| | |
|---|----|
| 1. Introduction | 7 |
| 1.1 Background | 8 |
| 1.2 Age of Arctic Ocean (AO) sediments and AO reduced basin margins | 10 |
| 1.3 Seismic studies of the area | 11 |
| 1.4 Continental and oceanic parts on YP | 12 |
| 1.5 West Spitsbergen Current..... | 13 |
| 2. Materials and Methods..... | 15 |
| 2.1 Data Acquisition | 15 |
| 2.2 Chirp Echo Sounder..... | 15 |
| 2.3 Post Processing | 16 |
| 2.4 Horizontal and vertical scaling in seismic profiles | 18 |
| 3. Results..... | 20 |
| 3.1. Chirp Profile Description | 20 |
| 3.2. The major findings of this study were the following: | 20 |
| 3.3 Acoustic facies description..... | 30 |
| 3.4 Crossing Profiles..... | 34 |
| 4. Discussion..... | 35 |
| 4.1 Discussion for profiles..... | 35 |
| 4.1.1 Iceberg Ploughmarks..... | 36 |
| 4.1.2 Erosional Unconformity | 36 |
| 4.2 Facies Discussion..... | 42 |
| 4.3 Age Control | 42 |
| 6. References | 48 |
| 7. Appendix | 53 |

1. Introduction

The Arctic Ocean plays a major role in the late Cenozoic global climate system because a significant part of the world's oceans dense cold bottom waters have their origin in the Nordic seas (Matthiessen et al., 2009). The production of these bottom waters drives the thermohaline circulation that controls heat transfer and climate. The bow-shaped Yermak Plateau (YP) is situated on the northeastern part of the Barents Shelf. The Yermak Plateau is northernmost plateau of the Eurasian plate, and is surrounded by the deep Nansen Basin to the north and northeast, the Sophia Basin to the east, the Fram Strait to the west and the Svalbard archipelago to the south (figure 1). The YP is separated from the Northern Svalbard margin to the east by huge Sophia Basin. The water depth ranges nearly 700-800 m over large parts, but at the central part on basement heights, is as shallow as 400 m (Gebhardt et al., 2011).

Seismic stratigraphy has long been used to illustrate the temporal and spatial evolution of ocean basins and their sedimentary cover. However, ground truthing of interpretations by subsurface sampling or correlation to outcropping sequences remains a critical step in developing these interpretations. Ground truthing not only provides necessary age control for recognized reflectors but also provides insights into the environmental conditions that generate variations in the physical properties of sediments.

Geologic models of the Arctic Ocean remain limited by the few available cores required for ground truthing and relatively sparse seismic data coverage attributable to the challenges of surveying under extreme ice conditions. Earlier marine geological and geophysical investigations have shown evidence for the former presence of grounded ice on the Yermak plateau, together with seafloor ploughmarks produced by deep-keeled icebergs. However, both the timing and interpretation of these events has been difficult to constrain (Kristoffersen et al., 2004).

This study presents new high resolution geophysical mapping of the seafloor morphology and shallow sedimentary stratigraphy and structures of the Yermak Plateau (YP) based on chirp sonar profiles. The main aim of this study is to produce a suite of geological maps and stratigraphic profiles that are used to geologically interpret the uppermost sediment stratigraphy and the bathymetry of the area. About 1270 km of chirp data were collected from the YP and adjacent basins providing new insight into sediment stratigraphy and the accompanying depositional history. In addition, the density and velocity data from the ODP leg 151 core 911A and 22JPC (The Healy–Oden Trans-Arctic Expedition (HOTRAX'05) 80° 29.386 N and 07° 46.141E (PANGAEA database, 2013)) from the YP are re-examined in the context of our high resolution geophysical data in order to make a correlation to the acoustic profiles.

1.1 Background

The Yermak Plateau is located on the eastern side of the Fram Strait, the main gateway for the transfer of ice and water between the Arctic Ocean and the North Atlantic during the Quaternary (Dowdeswell et al., 2010). Dowdeswell et al. (2010) proposed that ice sheets have advanced across the plateau only occasionally during the Quaternary, suggesting that the YP was inundated by ice only during the most extensive glaciations. Earlier marine geological and geophysical investigations by Vogt et al. (1994) and Flower (1997), have shown evidence for the former presence of grounded ice on the YP, together with seafloor ploughmarks produced by deep-keeled icebergs, but constraining the timing and interpretation of these events have proven difficult.

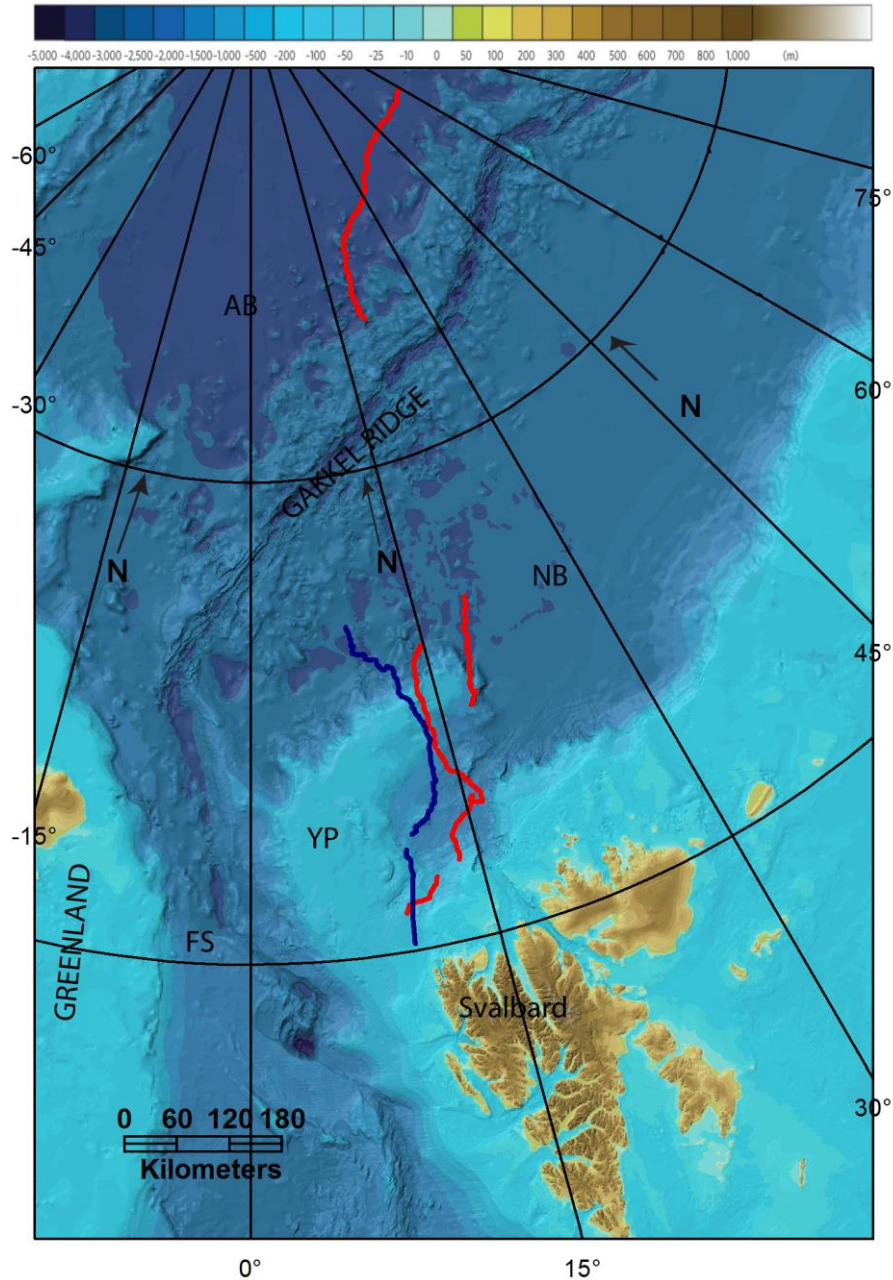


Figure 1. Three dimensional visualization of the Yermak Plateau and northern Svalbard margin, viewed from the south (darker colors represent deeper water) Red lines shows LOMROG II cruise whereas blue lines shows AGAVE cruise data used in this study. AB = Amundsen Basin, YP = Yermak Plateau, FS = Fram Strait, SB = Sophia Basin, NB = Nansen Basin (displayed on an annotated version of the IBCAO v.3 from Jakobsson et al. 2012).

1.2 Age of Arctic Ocean (AO) sediments and AO reduced basin margins

Jakobsson and Polyak (2011) highlighted that the age of most AO sediments is still tentative, especially for older strata. The Beaufort Gyre circulation and North American ice sheet impact predominantly effects the Western AO palaeoenvironments during most of the Middle-Late Quaternary (last ca. 0.5-0.7 Ma). According to Jakobsson and Polyak (2011), the age of sediment cores from the central AO generally does not reach to the base of Quaternary.

The AO turned into a smaller basin due to sea level falls during glaciations. With shallow and broad continental margins covered or exposed by ice sheets, riverine fluxes diminished, and connections to other oceans were limited to the Fram Strait alone. In fact, the wide and relatively shallow Arctic shelves occupy more than half of the Arctic Ocean area, implying that it was more than 50% smaller during peak glacial times. Jakobsson and Polyak (2011) also highlighted the presence of extensive ice shelves during the Quaternary glaciations similar to the present Antarctic ice shelves. These kinds of environment affect the biotic, hydrographic and sedimentary conditions in the ocean. Accordingly, sediment records from the AO shows cyclically alternated layers of distinct lithological, palaeobiological and chemical characteristics. Three major sediment types can be distinguished in a typical Arctic sediment core, deposited during interglacial/interstadial, deglacial (iceberg dominated), and full glacial environments. Also the severe fossil dissolution in Eurasian Basin sediments turns the correlation between the western and eastern Arctic Ocean very difficult. Various chronostratigraphic issues got further complicated the Arctic environments because of the principal differences in ocean circulation, sediment provenance and severe fossil dissolution in Eurasia Basin sediments. The development of independent age control from both Amerasian and Eurasian Basins as no single site can represent the entire Arctic Ocean, a reason for lacking of long stratigraphic records except Arctic Coring Expedition (ACEX) (Polyak., and Jakobsson., 2011).

1.3 Seismic studies of the area

Geissler and Jokat 2004 described three seismic units (YP-1, YP-2 and YP3) on the southern Yermak Plateau (profile AWI-99155; figure 2). Unit YP-1 consists mostly of parallel layers and graben infill with P-wave velocities ranging from 2.4 up to 4.2 km/s. Unit YP-2 consists of a thick sequence of sub parallel continuous reflectors and has its greatest thickness at the southwestern end of profile AWI-99155. To the northeast (shot point 1750, figure 2), this unit thins rapidly before it becomes thicker again, P-wave velocities for unit YP-2 from Sonobuoy measurements range between 1.9 and 2.4 km/s. The boundary to the overlying unit YP-3 represents an erosional discordance in the southwest. Unit YP-3 has a transparent reflection character with some continuous reflectors beneath the top of the Yermak Plateau (Nansen Bank). Further to the northeast, YP-3 is an acoustically fine layered sequence. YP-3 shows minimum thickness beneath the top of the Yermak Plateau (fig. 3a, shot point 2700). It thickens towards the southwest as well as in the northeast. P-wave velocities in the unit are between 1.7 and 1.8 km/s. P-wave velocities within the basement of YP are 5 km/s (SB9926) and 4.6 km/s (SB9926).

The seismic stratigraphy of the western Svalbard margin and the western Barents Sea reveals a prominent reflector known as the upper regional unconformity (URU) (Flower, 1997). This indicates that both Svalbard and Barents Sea ice sheets underwent a major transition in glacial sedimentation from net erosion to net deposition during the mid-Quaternary. In contrast to the disturbed sedimentation due to the Barents Sea ice sheets, the over-consolidated section on the Yermak Plateau experienced continuous sedimentation which suggests a decrease in Svalbard ice sheets grounding after ca. 660 ka (Flower 1997).

1.4 Continental and oceanic parts on YP

The YP in the north and the Spitsbergen plateau (SP) in the west have completely different origins and structures (Baturin et al., 1994). The southern part of the SP (south of 82° N), has a structure identical to most marginal plateaus on passive margins, with the main part underlain by continental crust (figure 2), and developed as a result of stretching during the rifting phase within the Eurasian Basin area. The northern part is mainly underlain by oceanic crust and developed primarily as a result of accumulative processes during the drift phase.

The southern and northwestern part of the YP is, on the other hand most probably of continental origin, whereas the northeastern, least explored part, which is characterized by strong magnetic anomalies, might consist of transitional or even oceanic-like crust (Jokat 2008).

Engen et al. (2009) studied the seismic stratigraphy and sediment thickness of the Nansen Basin, Arctic Ocean and recognized and correlated four Cenozoic seismostratigraphic units (NB-1 to NB-4) to previously published stratigraphic schemes. The first seismic stratigraphy for the Nansen Basin at ice drift station FRAM-IV based on multichannel seismic profiles on the northern slope of YP was published by Kristoffersen and Huseby (1985). Engen et al. (2009) discussed the Hinlopen margin and the inner YP area by using the study of Geissler and Jokat (2004) on the basis of Sonobuoy and gravity data, in which they proposed three-unit stratigraphy correlated to the ODP sites 910 and 911, to contribute in the establishment of the regional seismic stratigraphy and provide at least constraints for the upper sedimentary column on the YP.

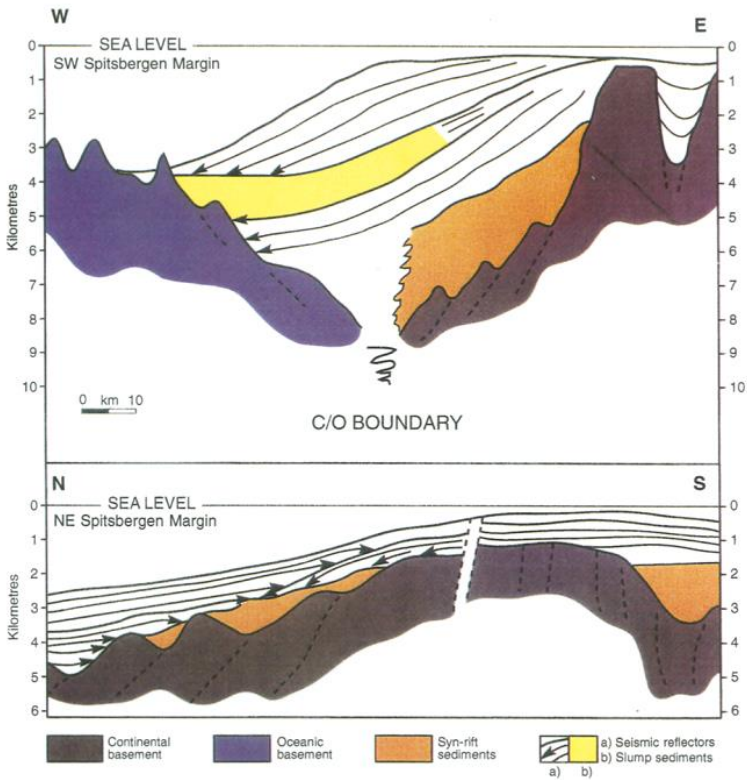


Figure 2. Schematic geological cross-sections of a) SW-Spitsbergen Margin and b) NE-Spitsbergen Margin (Baturin et al. 1994).

1.5 West Spitsbergen Current

The West Spitsbergen Current (WSC) is the northernmost extension of the Norwegian Atlantic Current. It flows pole ward through the eastern Fram Strait along the western coast of Spitsbergen. A mainly barotropic current, the WSC appears to be predominantly steered by the bathymetry. It is quite narrow and strong about 100 km wide and is confined over the continental slope, where it reaches its maximum current speed of 24 to 35 cm s⁻¹ at the surface (Piechura et al. 2001). Because it transports relatively warm (6 to 8°C) and salty (35.1 to 35.3 psu) Atlantic Water, the WSC keeps eastern Fram Strait and adjacent western border of the Barent Sea area free of ice (Piechura et al. 2001). The WSC follows the continental slope which splits at the junction of the YP and the Spitsbergen continental shelf (Cokelet et al., 2008). The upper 500 m of surface

waters are deflected east by the Coriolis force to flow to the north of Svalbard; this water mass is termed the North Spitsbergen Current (NSC). The remaining deeper waters of the WSC continue north, flowing along the margin of the Yermak Plateau as the Yermak Branch (YB) (Howe et al., 2008).

Cokelet et al., 2008 found Atlantic water in the upper 500 m depth of all of the five interpreted oceanographic sections. The WSC in the Fram Strait at 78°N forms the Atlantic layer (AL), characterized by a temperature of 0°- 2°C and salinities of 34.7- 35 psu, which passes into Arctic Ocean along the northern continental slope of Svalbard. The Yermak branch moves northwest towards the Yermak Plateau and loses its Atlantic water qualities rapidly, while the Svalbard branch supplies a major part of the Atlantic water in the form of the Atlantic layer into Arctic Ocean. The Atlantic layer is between 100-200 and 600-800 m deep with temperature fluctuations in its main core from 3°C to 4.5°C at 100 to 400 m water depth (Slubowska et al., 2005). The velocity of the WSC along the margin (500-1500 m depth) ranges between 9 to 16 cm/sec, whereas the relatively slower Yermak Branch (YB) ranges between 1 to 3 cm/sec (Howe et al., 2008).

2. Materials and Methods

2.1 Data Acquisition

The geophysical data presented in this thesis were primarily collected with Ice Breaker Oden's hull mounted multibeam echo sounder (EM 120) and sub-bottom profiler (EM 122), during two expeditions (Jakobsson et al, 2010):

- AGAVE (Arctic Gakkel Vents Expedition) July 1st - August 11, 2007 and;
- LOMROGII (Lomomosov Ridge off Greenland) July 31 – September, 2009.

2.2 Chirp Echo Sounder

A system integrated SBP 120 chirp echo sounder was used to acquire the high resolution sub-bottom profiles during both expeditions. During the cruises a linear FM pulse with a bandwidth of 2.5 – 7 kHz was used, which is capable of vertical resolutions of up to 0.3 ms (up to 11 simultaneous beams in a across the ship's keel direction, each having a beam width of 3 degrees). The SBP 120 utilizes the same receiving array as the EM 120, and a separate transmission array attached parallel to the EM 120 transmission array (fig. 8) (AGAVE cruise report, 2007). This multibeam system was upgraded to Kongsberg's EM 122 prior to the LOMROG-II expedition (Jakobsson et al, 2010). The Seatex Seapath 200 heave, attitude and positioning system were used throughout the two expeditions (AGAVE cruise report, 2007).

The acoustic impedance of a rock is defined as the product of its density and seismic velocity. On striking of a seismic wave-front to a planar interface between rock strata with impedances I_1 and I_2 at normal incidence, the percentage of energy reflected (the reflection coefficient, RC) is given by the following equation:

$$RC = \frac{I_2 - I_1}{I_2 + I_1} \quad (1)$$

Acoustic impedance $z = \rho v$ (density * velocity)

Lower frequency signals penetrate deeper into the sediment due to higher energy, but the resolution of the signal will also be poorer due to the increased wavelength. Higher frequency signals cannot reach as deep, but will instead give high resolution data from the depth they penetrated i.e. good resolution of shallow sediment (Meridata, 2008).

2.3 Post Processing

Interpretation of the acoustic records was done as a desktop study, using the Meridata MDPS (post processing) system. To classify sediment structures, approximately 1270 km of high-resolution acoustic data (over 150 chirp profiles) was examined. The collected data from the penetrating echo sounder was treated in the Meridata software suite, using the program S.View to acquire an optimal set of post processing parameters for the seismic interpretation, and MDPS 5.1 for visualization and interpretation of acoustic units.

The interpretation procedure was performed in a few main steps:

The raw sub-bottom data files were exported to SEG-Y format using Kongsberg's SBP120 v. 1.6.4 software. The Kongsberg SEG-Y files were then converted to a "standard" SEG-Y format readable by MeriData using the dedicated program Read-SEG-Y (pers. comm. Tom Floden). The spatial maps within the study area were also created in GIS environment using Intergraph's Geomedia Professional, ArcGis and Quantum GIS, displayed using a WGS84 datum. A processing chain applied to the raw data including match filtering, time variable gain (TVG) and gain. The gain parameter was changed between different profiles when needed, but never within the same profile. Profiles are presented using a grey scale map (see figure A17 for Screen dump of Kongsberg's SBP120v1.4.6 with system settings).

To test the compatibility of different interpretations we integrated the interpreted seismic profiles into the 3D visualization software Fledermaus. We used Fledermaus professional was used to merge and edit the bathymetric surfaces and sub bottom profiles in to a 3D environment for analysis and presentation. As Fledermaus use a geospatial coordinate system based on vertical coordinates in meters, a two-way travel-

time to depth conversion had to be performed on all seismic profiles used in this study. This conversion was done using a sound velocity function of 1500 m/s for the entire marine geological column (water and sediments).

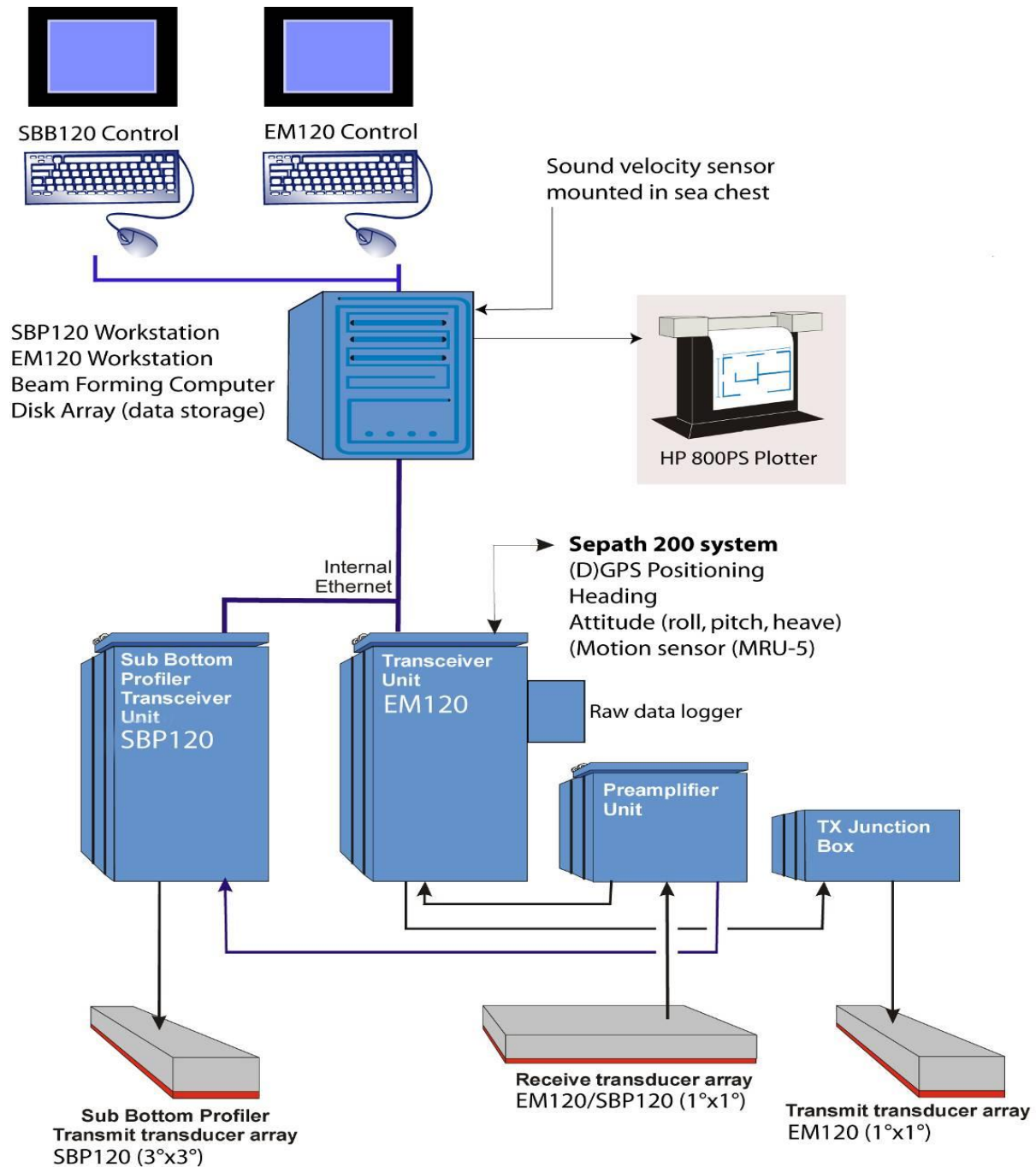


Figure 3. Schematic illustration of the EM120/SBP120 system installed on the Oden. The drawing is a modified version of Kongsberg's original (cruise report-2007).

Quantum GIS was used to geo-reference the seismic track lines for visualization. The International Bathymetric Chart of the Arctic Ocean (IBCAO.v 3) (Jakobsson et al, 2012) was integrated as a background to finally present a compilation of all track lines in relation to the regional bathymetry of the Arctic Ocean. The sections or type profiles were uniformly scaled in every section so that one second TWT time when measured and expressed in cm along the y-axis, could be shown consistently.

2.4 Horizontal and vertical scaling in seismic profiles

The vertical time scaling in the seismic profiles is fixed and independent of changes in sound velocity marked by scaling lines, normally printed 100 millisecond apart. It should be observed that 100 ms is the two way travel time of the seismic signal equaling to 75 m at a sound velocity of 1500 m/s.

The horizontal scaling, on the other hand, is dependent on variations in the ship's speed (Floden et al, 2001). Thus, the horizontal distance in the seismic profiles is indicated by successive position markings. Each position fix is assigned a time stamp that is marked on the recording.

Additional software used for better data visualization and analysis were Global Mapper, Grapher (drawing the core data), Chircor (to draw the synthetic seismogram for the ODP hole 911A Leg 151 core data, see figure A18) according to Forno and Gasperini 2008, Matlab (to filter core data i.e. resampling of density and P-Wave data at an interval of 0.5 cm throughout whole data), Adobe Illustrator CS5, and Adobe Photoshop CS5.

The interpretation procedure was performed for major reflectors at crossing profiles in two dimensions by juxtaposing the interpreted seismic sections and tying up corresponding reflectors. Subsequently, the key crossing profiles were visualized in the 3D environment Fladermaus. This allowed further control on spatial compatibility between closely surrounding seismic profiles.

Table 1. EM120, EM122 and SBP120 technical specifications (LOMROG-II cruise report, 2009).

| | |
|--------------------------------------|---|
| EM120 (1°) | Depth range: 20 to 11000 m Swath width: up to 5 times water depth (ice protection windows reduce this to ca 4 times the water depth) Beam width: 150°x1° Beams: 191 covering a sector up to 150° Frequency: 12 kHz |
| EM122 (1°) | Depth range: 20 to 11000 m Swath width: up to 25% better than EM120 Beam width: 150°x1° Beams: 288 simultaneous beams covering a sector up to 150° Frequency: 12 kHz (chirp mode and dual swath capability) |
| SBP120 (3°) | Frequency range: 3-7 kHz, chirp Vertical resolution: 0.35 ms Horizontal resolution: 3°x3° Integrated with EM120 by using the same receiving transducer array |
| Positioning and motion sensor | Seapath 200 (for more information see: http://www.seatex.no/vesselrefsys/seapath200/seapath200.html) MRU5 (motion reference unit) Heading accuracy: 0.05 RMS (4 m baseline) Roll and pitch accuracy: 0.03 RMS for ±5° amplitude. Heave accuracy: 5 cm or 5% whichever is highest Positioning accuracy: (best case) 0.15 m RMS or 0.4 m (95% CEP) |

3. Results

The analysis of 1270 km (141) sub-bottom profiles (LOMROG II and AGAVE expeditions) and multi-beam bathymetry from both expeditions have provided new images of high resolution seafloor morphology and shallow sediment structure on the YP at few locations.

3.1. Chirp Profile Description

The investigation of the seafloor morphology and acoustic stratigraphy of the Yermak Plateau has been on the basis of high resolution geophysical evidence derived from multibeam bathymetry and sub bottom acoustic profiling. The stratigraphy of ODP Leg 151 site 911A core data and HLY0503-22-JPC core data from the Yermak Plateau re-examined in the light of the geophysical data.

3.2. The major findings of this study were the following:

After processing a total of 141 acoustic profiles data spread out over the study area, I have used five type profiles (A - A', B - B', C - C', D - D' and E - E') containing 21 acoustic profiles in this study, see Figure 5 for location on the Yermak Plateau (YP). There is not much in all remaining data which can be utilized for more type profiles for further processing and investigation. The data quality is very low due to bad ice conditions during the data acquisition and could not able to see clear reflectors in all profiles even after using various filters in different software packages. It's not possible to create an acoustic stratigraphy for the entire study area. Type profiles A - A' & E - E' are from the eastern part of Yermak Plateau (YP) slopes, B - B' & D - D' are from the south eastern shallow part of YP and C - C' from the northern north eastern tip of YP, see Figure 5 for the location of all profiles. In all profiles, length is in kilometers (km) and depth is in both meters (m) and millisecond (ms) at left and right side of the profiles respectively.

The detailed description of these five type profiles is written below:

1. A - A' (Figure 6): 60 km long, slopes down from north to south and shows parallel strong alternating dark and light acoustic reflectors. Acoustic

- penetration varies from 20 m at steeper slopes to 70 m at stable slopes. The profile is at water depth ranging from 1350 to 2175 m.
2. B - B' (Figure 7): south to north 60 km long profile shows more features in the study area. The acoustic penetration varies from 20 to 50 m with parallel but not uniformly distributed reflectors throughout the type profile. Firstly, there are three iceberg ploughmarks, one at 540 m water depth at the southern part of the profile (Figure 7 part "a" at 80 3.970 N 9 54.250 E) and the other two "b" (80 32.659 N 10 16.257 E) and "c" (80 34.550 N 10 15.200 E) at the northern part at 790 m and 830 m water depth respectively. Secondly, there is an erosional surface in part 'd' (80 9.870 N 9 56.865 E) underlain by an acoustically transparent zone. Thirdly, at part "e" of the Figure 7 (80 23.250 N 10 5.150 E to 80 27.056 10 9.931 E), the acoustic penetration depth decreases from 50 m to 20 m up to 6 km length. After this patch acoustic thickness again increases and acoustic thickness reached to about 50 m again as the similar previous pattern before the thin patch.
 3. C - C' (shown in Figure 6): 25 km long northwest to southeast profile in a water depth of 1680 to 1900 m. This profile lies on the north eastern most part of the YP. Apart from the top strong acoustic reflector at the seafloor, acoustic penetration is very low in the profile. At stable topography there is a disturbed internal acoustic reflector at places at about 10 m below seafloor.
 4. D - D' (shown in Figure 9): 125 km north to south long type profile in a water depth of 675 - 2175 m, lies at the southern part of YP (crossing B - B' profile) with parallel to sub-parallel reflectors in a 20 to 50 m thick sequence. The profile is further divided in to three important parts a, b and c. At part "a" there is a sharp change in the acoustic character where acoustic thickness drops to about one third of the 50 m thick acoustic sequence with uneven parallel to sub-parallel internal acoustic reflectors.

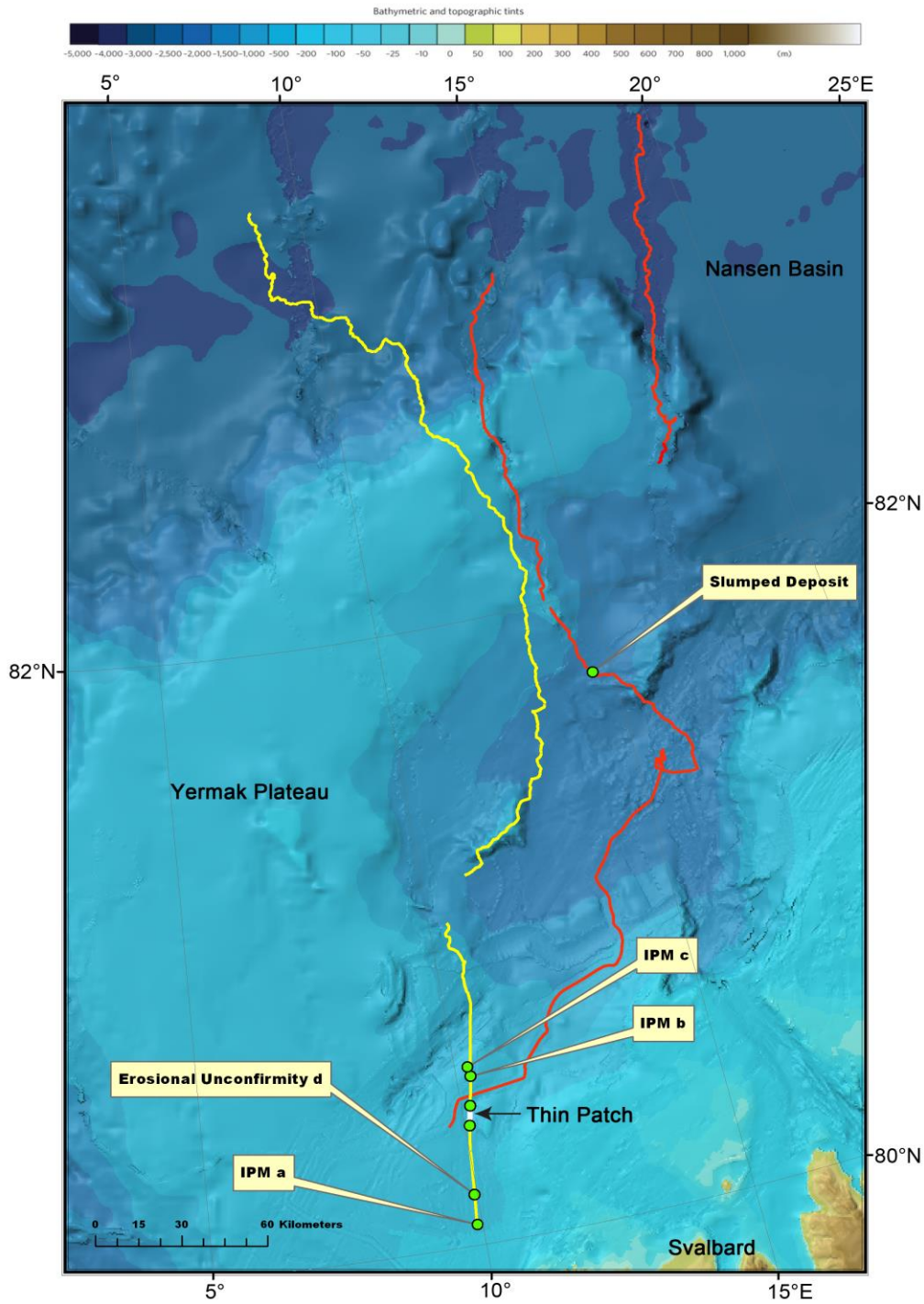


Figure 4. A compilation of all the interpreted seismic track lines displayed on an annotated version of the IBCAO v.3 from Jakobsson et al. 2012. Red lines shows LOMROG II cruise whereas yellow lines shows AGAVE cruise data used in this study along with IPM, erosional unconformity and thin patch (white line). (Darker colors represent deeper water) YP = Yermak Plateau, NB = Nansen Basin, IPM= iceberg ploughmarks.

The thin acoustic sequence with missing internal reflectors continue till 20 km length from south to north and then acoustic thickness gradually increased with parallel well stratified acoustic sequence of up to 50 m thick. At part “b”, internal acoustic reflectors getting thin again and dies out. After that the thin acoustic sequence of about 20 m thickness with no internal acoustic reflectors continues to the end of the profile. There are a few light character sub-bottom lenses at part “c”.

5. E - E' (Figure 10): 40 km long northwest to southeast profile at 1500-2400 m water depth. This very low quality profile with very high elevation slopes show varying acoustic penetration lies on the eastern slope (near to A - A') of YP. At the south eastern part, there is about a ~ 5 km long thick lighter layer at part “a” (81 44.714 N 14 33.765 E) (southeastern side) with visible underlying acoustic reflectors.

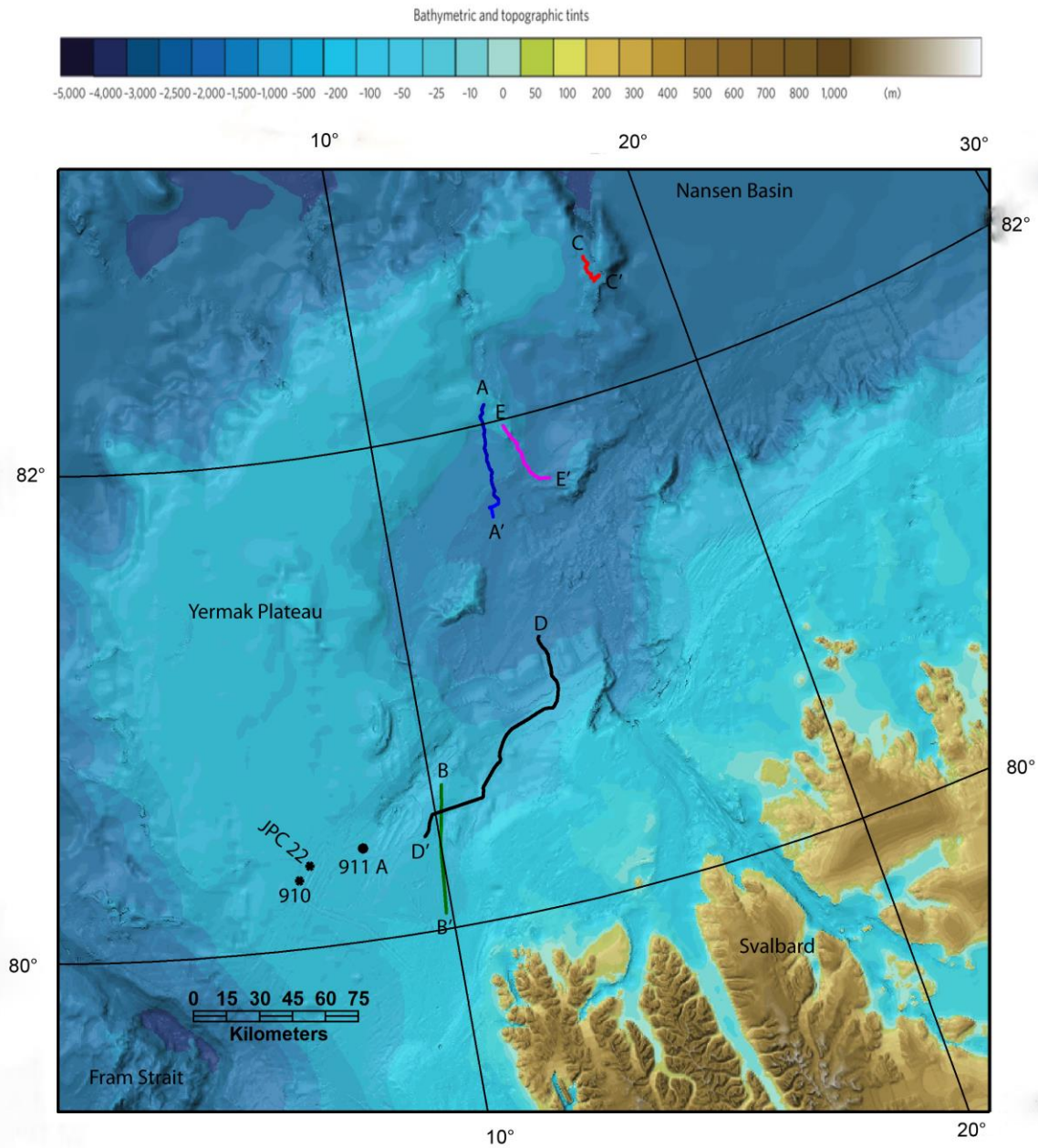


Figure 5 . A detailed location map of the acoustic profiles track lines, showing the five type profiles (AA'-EE') coverage over the bathymetry (IBCAO v.3) in the investigation area. Black dots show the ODP core sites 910, 911A and JPC 22. YP = Yermak Plateau, FS = Fram Strait, SB = Sophia Basin, NB = Nansen Basin

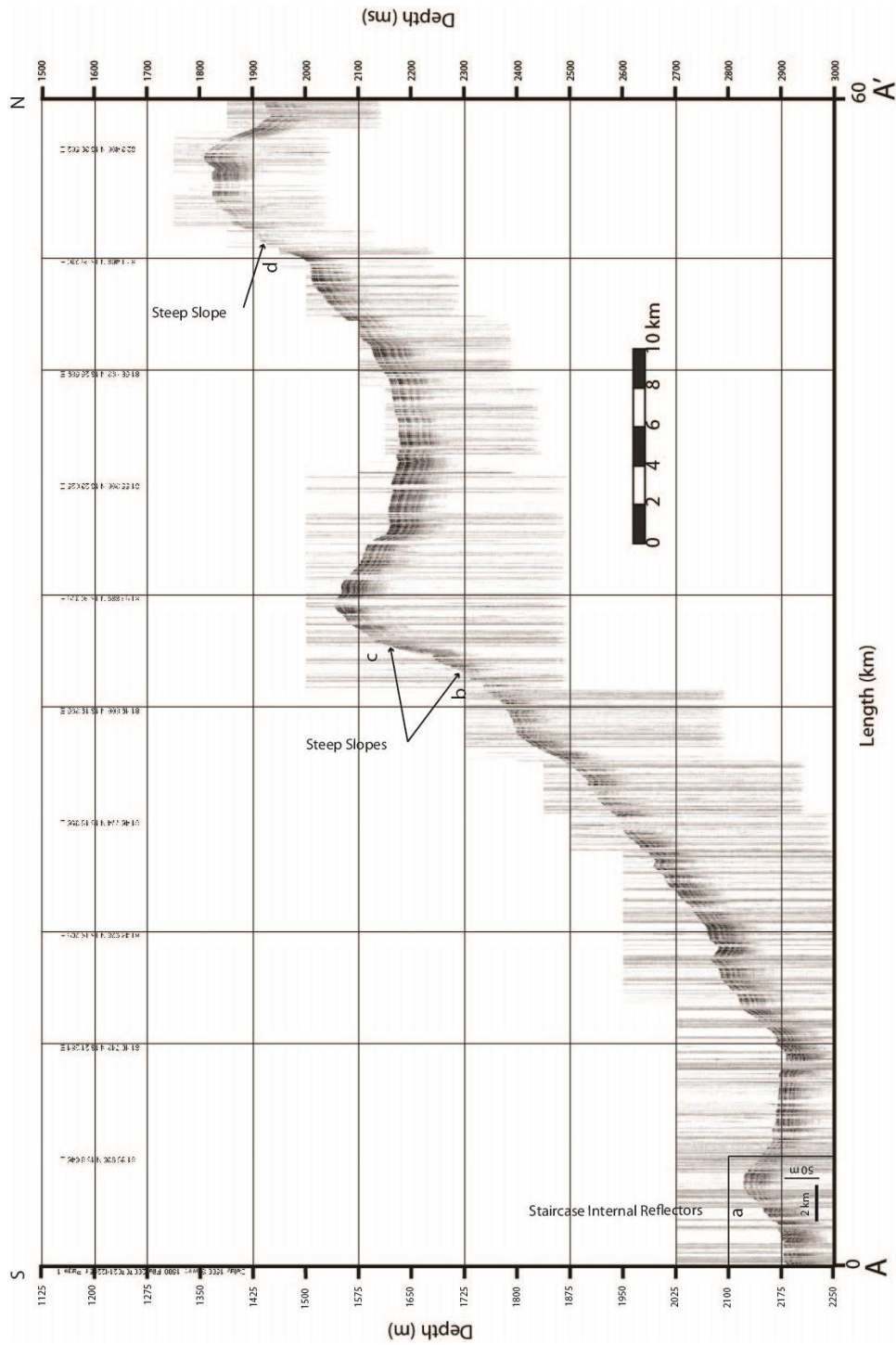


Figure 6. Chirp sonar records for profile A - A'. The location of the profile is marked by green line in Figure 5. Water depths are calculated using an average sound velocity of 1500 m/s for water column and sediments. Depth shows both in meters (m) and milliseconds (ms) on left and right side of profile, respectively.

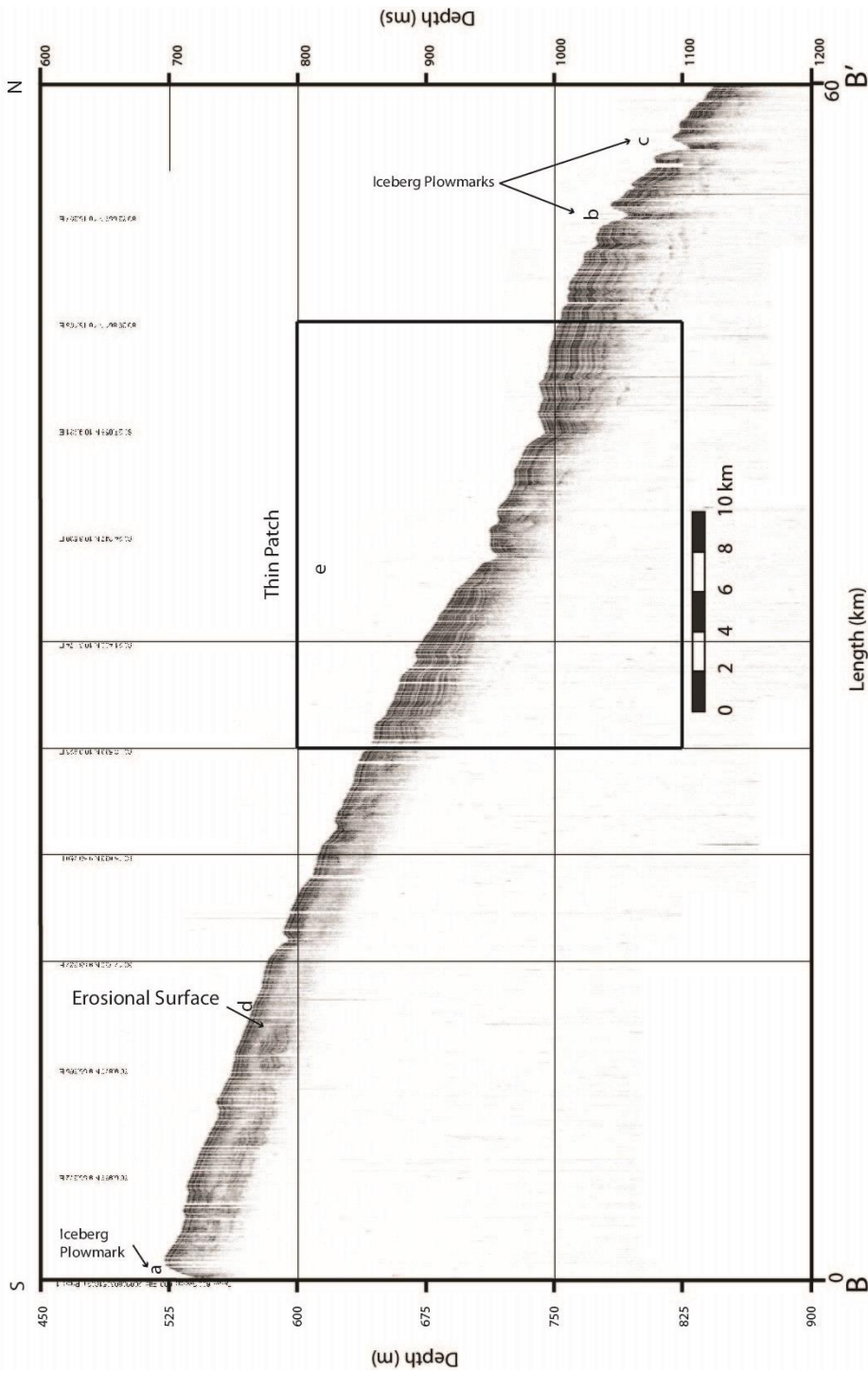


Figure 7. Chirp sonar records for profile B - B'. The location of the profile is marked by green line in Figure 5. Water depths are calculated using an average sound velocity of 1500 m/s for water column and sediments. Depth shows both in meters (m) and milliseconds (ms) on left and right side of profile, respectively.

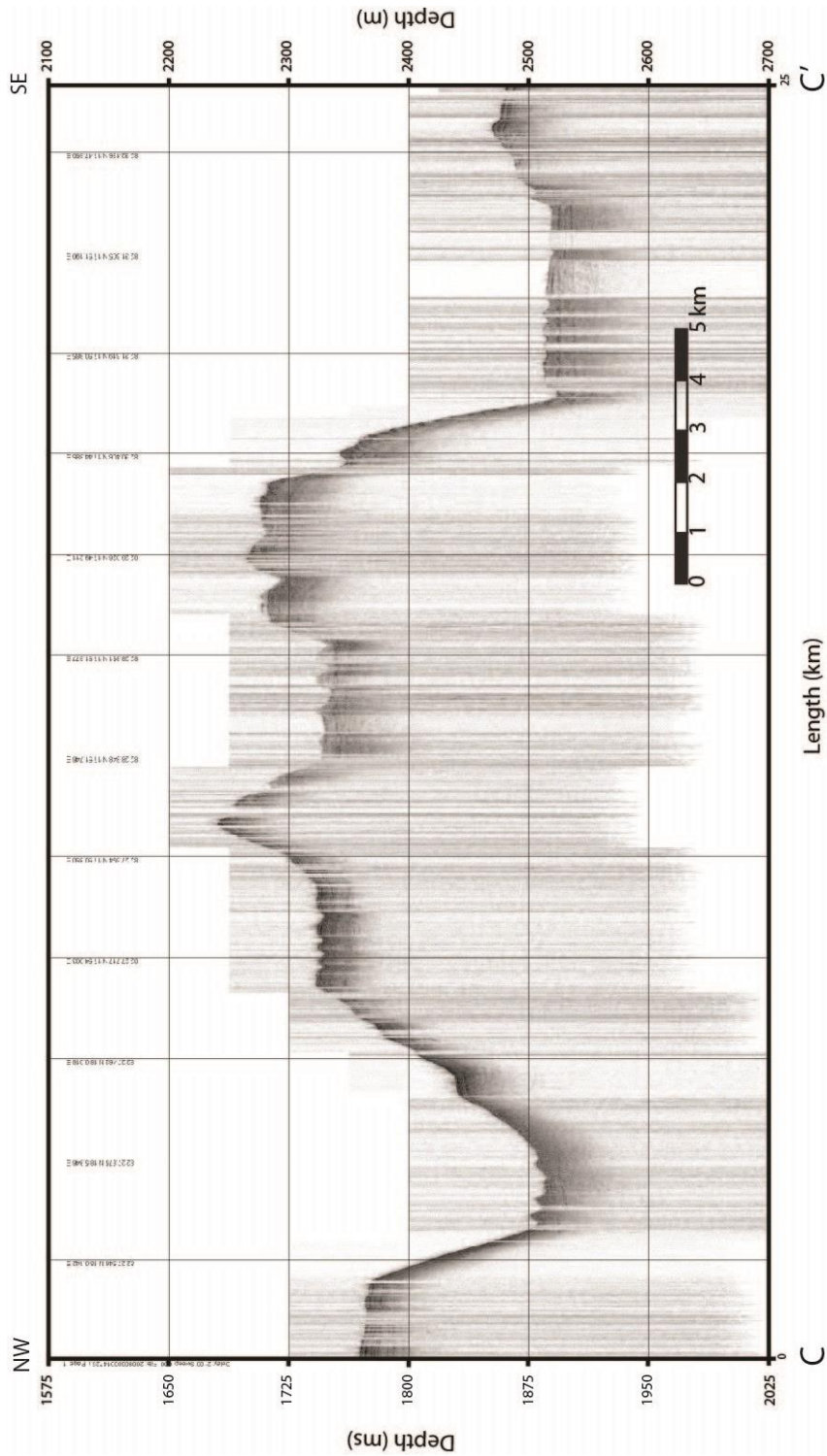


Figure 8. Chirp sonar records for profile C - C'. The location of the profile is marked by green line in Figure 5. Water depths are calculated using an average sound velocity of 1500 m/s for water column and sediments. Depth shows both in meters (m) and milliseconds (ms) on left and right side of profile, respectively.

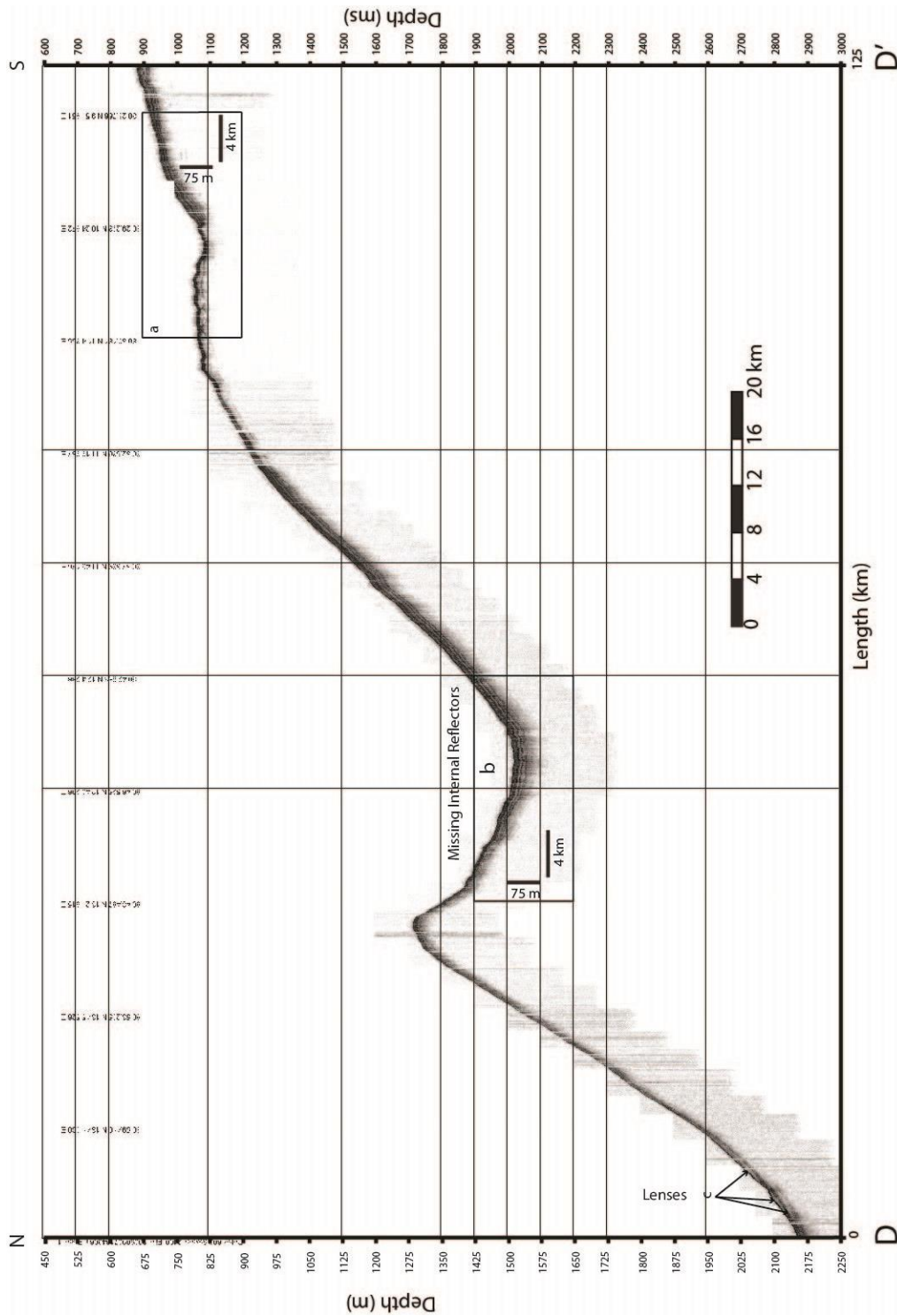


Figure 9. Chirp sonar records for profile D - D'. The location of the profile is marked by green line in Figure 5. Water depths are calculated using an average sound velocity of 1500 m/s for water column and sediments. Depth shows both in meters (m) and milliseconds (ms) on left and right side of profile, respectively.

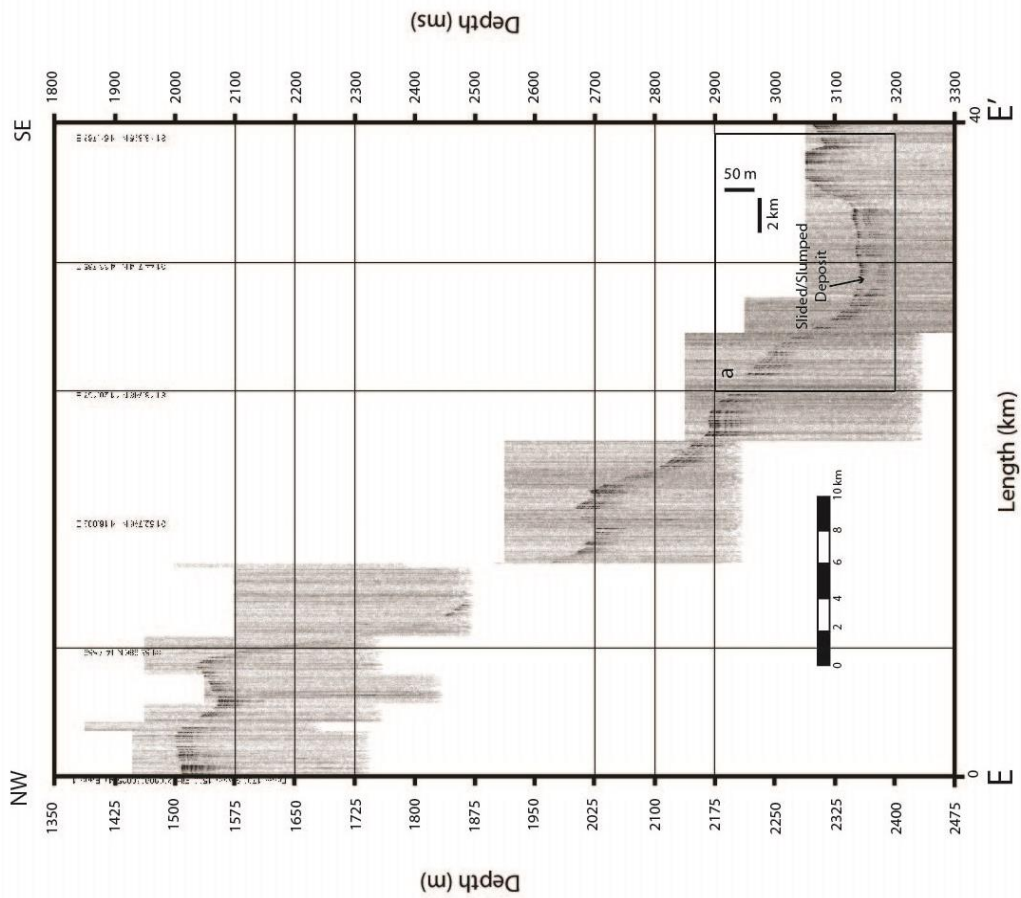


Figure 10. Chirp sonar records for profile E - E'. The location of the profile is marked by green line in Figure 5. Water depths are calculated using an average sound velocity of 1500 m/s for water column and sediments. Depth shows both in meters (m) and milliseconds (ms) on left and right side of profile, respectively.

3.3 Acoustic facies description

Acoustic type facies can be used to illustrate the different combinations of acoustic facies over a region of the sea floor. A short description about the major acoustic facies shift in reflector character in the 141 sub bottom profiles from the AGAVE and LOMROG expeditions is as under:

Four major acoustic facies have been differentiated in the sub bottom profiles in my study area of the Yermak Plateau on the basis of prominent and transparent acoustic character with disturbed and stratified strata (see Figure 11b for the location of all described facies).

1. This facies (F1) multiplies characterized by many sub-bottom acoustic uneven reflectors which are parallel to sub-parallel to the seafloor. Thickness varies from 20 - 50 m at 520- 840 m water depth, in type profile "A - A" in Figure 6 at the start of AGAVE expedition data in Figure 4 on the Yermak Plateau. The upper 20 m part shows parallel layering with acoustically semi-transparent basement except at 640 - 710 m and 740 - 780 m seafloor depth where the upper layered part thickened to about 45 m (e.g. profile-102 or Figure 11a part F1 and at location "a" in Figure 11b).
2. The 2nd facies (F2) shows parallel acoustic reflectors, thin packages 10 to 50 m thick, bound by very prominent upper and lower reflectors with dark and lighter layers of various thicknesses. This facies found at seafloor depths of 680 to 2100 m with very steep slopes in this study area. This facies is present in both expeditions (AGAVE and LOMROG II) track area (e.g. profile-818) Figure 11a F1, at location "e" in Figure 11b.
3. The 3rd facies (F3) is divided into two parts; the first part dominated the seismic stratigraphy in the LOMROG expedition area and represents stratified strong and parallel dark and light layers with very little disturbances throughout the whole data north of the YP in Nansen Basin. Facies F3 (continuous horizontal

reflectors) was found mostly deeper than 4000 m water depth but also found at relatively shallower water depths with disturbed steep slopes. The thickness of the acoustic basement under this facies varies from 20 - 80 m and found at deepest horizons. The thickness of the dark and light layers also varies in Figure 11a, part F3, at location "d" in Figure 11b (e.g. profile-318).

A similar facies is a continuity of facies F3 but found at shallower depth, under 800-2000 m deep seafloor. The layering is almost parallel in this facies except at a few points where very weak layering was found (at location "b" in Figure 11b).

4. The 4th facies (F4) starts sharply in profile 303 at 1720 m depth and continues to 2600 m. A strong 10 m thick dark homogeneous layer with few weak internal acoustic reflectors thick but mostly acoustically transparent to semitransparent underlying material to the dark layer Figure 11a, part F4, at location "c" in Figure 11b (e.g. profile-306).

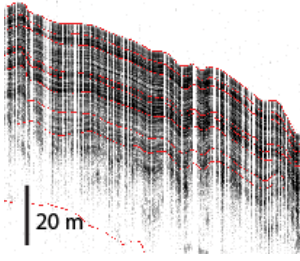
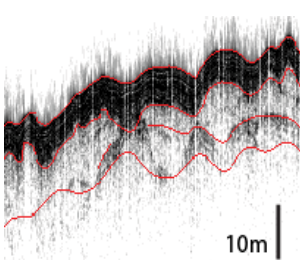
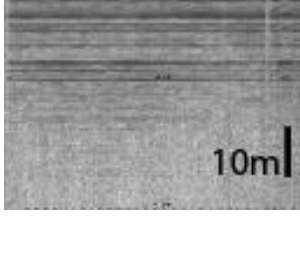

| Acoustic Facies | Example | Character |
|-----------------|---|--|
| F1 (102-005839) |  | <p>The internal reflectors are parallel - sub parallel to seafloor surface. The internal reflectors show slightly wavy pattern in most parts. This pattern is visible between ~ 500 - 800 m of the acoustic profile depth.</p> |
| F2 (818-215740) |  | <p>Acoustically stratified with very stacked strong acoustic reflectors at water depth of below 750 m. Internal acoustic reflectors are missing in this facies</p> |
| F3 (318-203643) |  | <p>Acoustically well stratified dark and light reflectors that are continuous, parallel to the seafloor surface. This facies consists of sheet like units of acoustically semitransparent to strong units. This pattern can be observed at deeper depths below 4000 m.</p> |
| F4 (306-042525) |  | <p>Acoustically transparent to semitransparent facies with a few irregular reflectors at places.</p> |

Figure 11a. Acoustic profiles showing different acoustic facies in the study area. See Figure 11b for location of all facies parts.

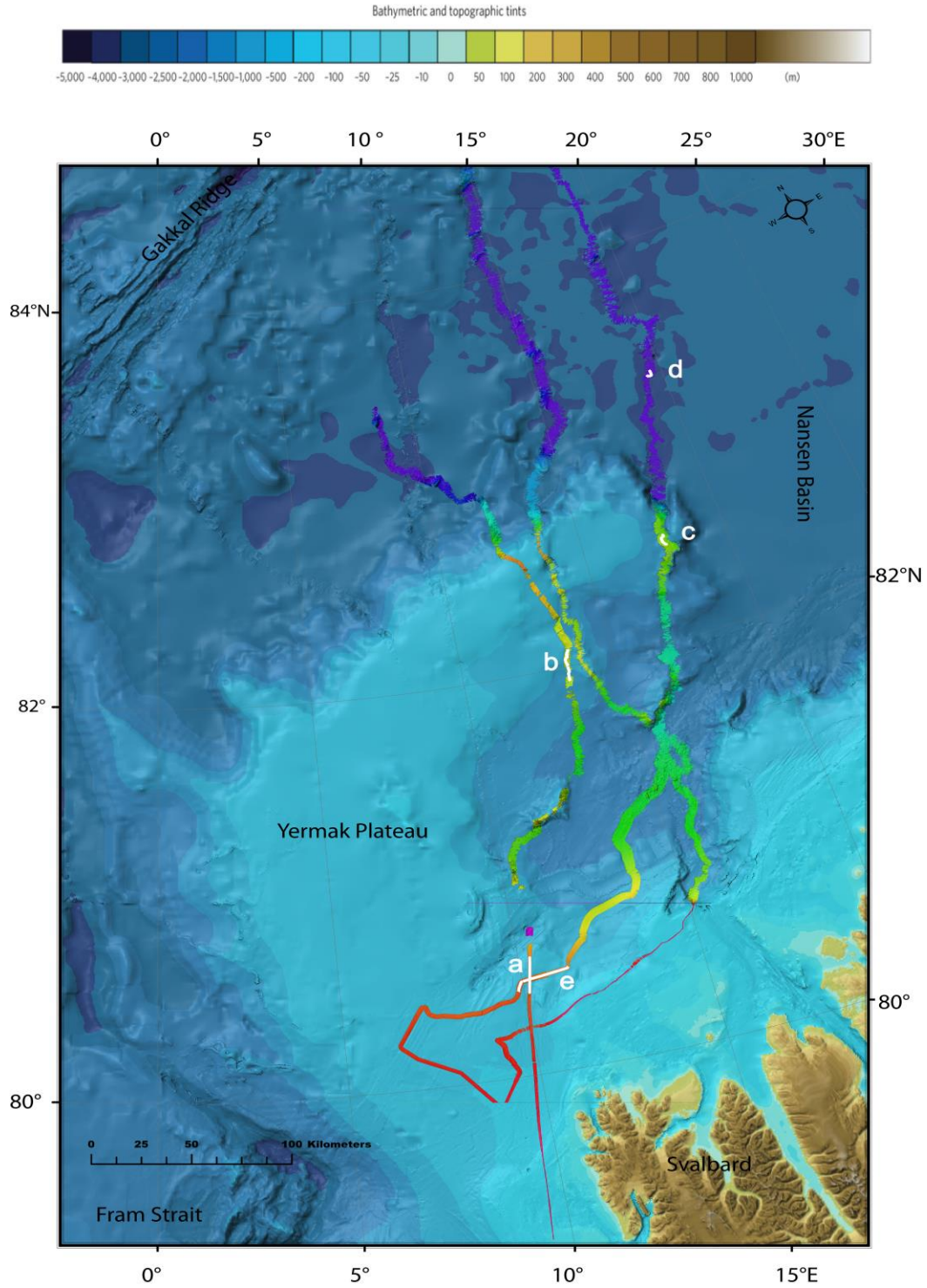


Figure 11b. White lines “a” to “e” shows location of the acoustic facies parts in the study area along with bathymetry (displayed on an annotated version of the IBCAO v.3 from Jakobsson et al. 2012).

3.4 Crossing Profiles

The acoustic crossing profiles are visualized in a 3D environment as vertical hanging sections (Figure 12). The correlation between the crossing point of profiles and extensions is then presented by juxtaposing the 2D interpreted (in meridata suite) sections. The chirp sonar profiles showing that the acoustically parallel to sub-parallel thick reflectors turns in to very thin sharply changed reflectors integrated with the bathymetric data (figure16). The location of the crossing profiles is indicated in Figure 4 (Red and Yellow lines crossing at bottom of the figure), .

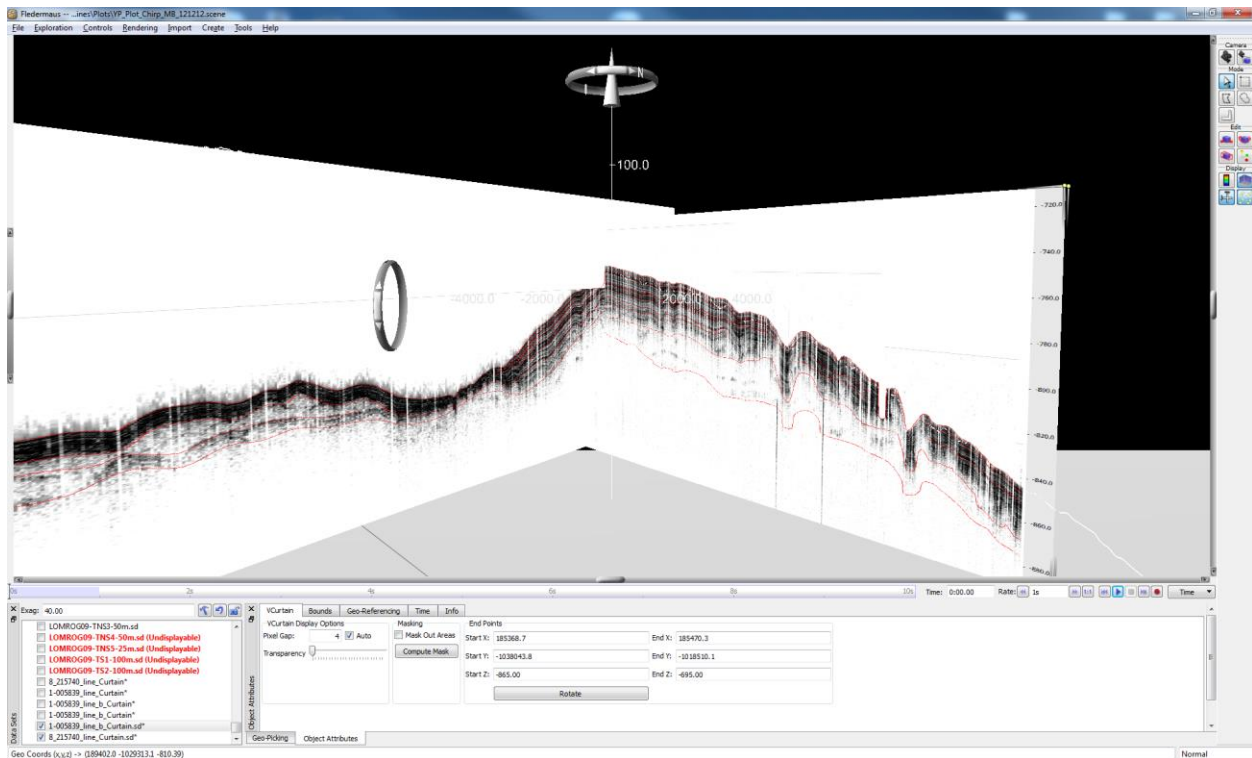


Figure 12. A 3D model showing interpretation of the acoustic reflectors of the crossing profiles at the southern YP crest. The location of the crossing profiles is indicated in figure 5 (Red and Yellow lines crossing at bottom of the figure).

4. Discussion

The Yermak Plateau is located relatively far away from any major sediment sources and therefore has the potential to preserve a much cleaner record of palaeoceanographic events, such as variation in sea ice and the flow of a slope current. Acoustic profiles indicate well-stratified sediments, which decrease in thickness significantly over short lateral distances down-slope directly adjacent to steep slopes. The overall character of the pattern is typical for marine drift deposits, which are controlled by the influence of bottom currents.

The distribution of the seismic lines and their observed structures is described here. The Yermak Plateau profiles display a variable acoustic character (Figure 11a). The plateau itself displays highly disturbed, parallel, well-stratified reflections, with an acoustic penetration of 20 to 70 m below the sea floor; this reflection is interpreted as a draped cover of fine-grained sediment subsequently disturbed by iceberg scouring. The iceberg scours extend to 830 m present water depth (Figure 7). The deeper (>1300 to 2300 m) slopes of the plateau display sub-parallel, well-stratified reflections downslope with acoustic penetration between 20 to 50 m. The reflections on the northern slope of the plateau, leading towards the Sofia Deep, display a subtle and irregular waveform which can be seen in Figures 8 and 12. These could be interpreted as either current-influenced features or as downslope movement of the thick sediment pile leading to creep on the slope. Combining the acoustic profiles with swath bathymetric data reveal different events marked by an erosional unconformity, slump deposit and iceberg ploughmarks all covered by later sedimentation.

4.1 Discussion for profiles

The reason for low acoustic penetration at steeper slopes could be low sediment accumulation with less stability which could cause relatively high sediment accumulation towards the deeper stable slope areas but all reflectors show layered structure (see Figure 6,A - A' profile). In part 'a' some staircase disturbed internal reflectors with dark and light parallel layers are visible, interpreted as glaciomarine deposits.

4.1.1 Iceberg Ploughmarks

The deepest iceberg ploughmark is about 500 m wide and 25 m deep, and is mapped on the southern YP at a depth of 830 m below present sea level (Figure 14). By analyzing the iceberg ploughmarks in the acoustic profiles (B - B' profile, Figure 7 part a, b and c), there occur sedimentation inside the all three ploughmarks, so the current dimensions for the ploughmarks are not true, affected by the later sedimentation.

The deepest iceberg ploughmark in the studied area (shown in Figure 7 and 14) at about 830 meter below seafloor, is probably the same one discussed by Vogt et al, 2011, they proposed that they were late Pleistocene products of calving of the Barents–Kara ice sheets into the Arctic Ocean. The Vogt et al. (1994) hypothesis that very large icebergs with draft of 300 to 700 m or more grounded in the Arctic Ocean, is supported by a 100 - 150 m lower sea level during the late Pleistocene glacials.

4.1.2 Erosional Unconformity

Different glacial events have affected the seafloor of the YP. An ice sheet grounded event that extends to 650 m present water depth. The erosional surface in B – B' part d (Figure 7) is underlying an acoustically transparent chaotic zone of about 15 - 20 m at 20 m below seafloor, which could be due to ice sheet grounding in the area. This grounding event is characterized by an erosional unconformity at 30 m depth below seafloor in this study area (Figure 7) and is overlain by an acoustically chaotic layer of roughly 15 to 20 m thickness interpreted as northern extension of diamicton described by Gebhardt et al. (2011) in the nearby area at the southern YP at about 80 ° N. This layer can be correlated to the overconsolidated sediments found at ODP Site 910 (due to the similar depths below seafloor) at a sediment depth at about 18 m depth below seafloor Figure 13. In Figure 13 the similar depths for the overconsolidated section can be seen in acoustic profile 121-231847 and AWI 20020390 profile. The oldest sediments just above the overconsolidated part are of late early Pleistocene age MIS 16/17 by means of oxygen isotope stratigraphy and provide a minimum age for the grounding event (Gebhardt et al, 2011).

Three possible explanations for the erosional event (Figure 7 part d) in the southern part of study area are:

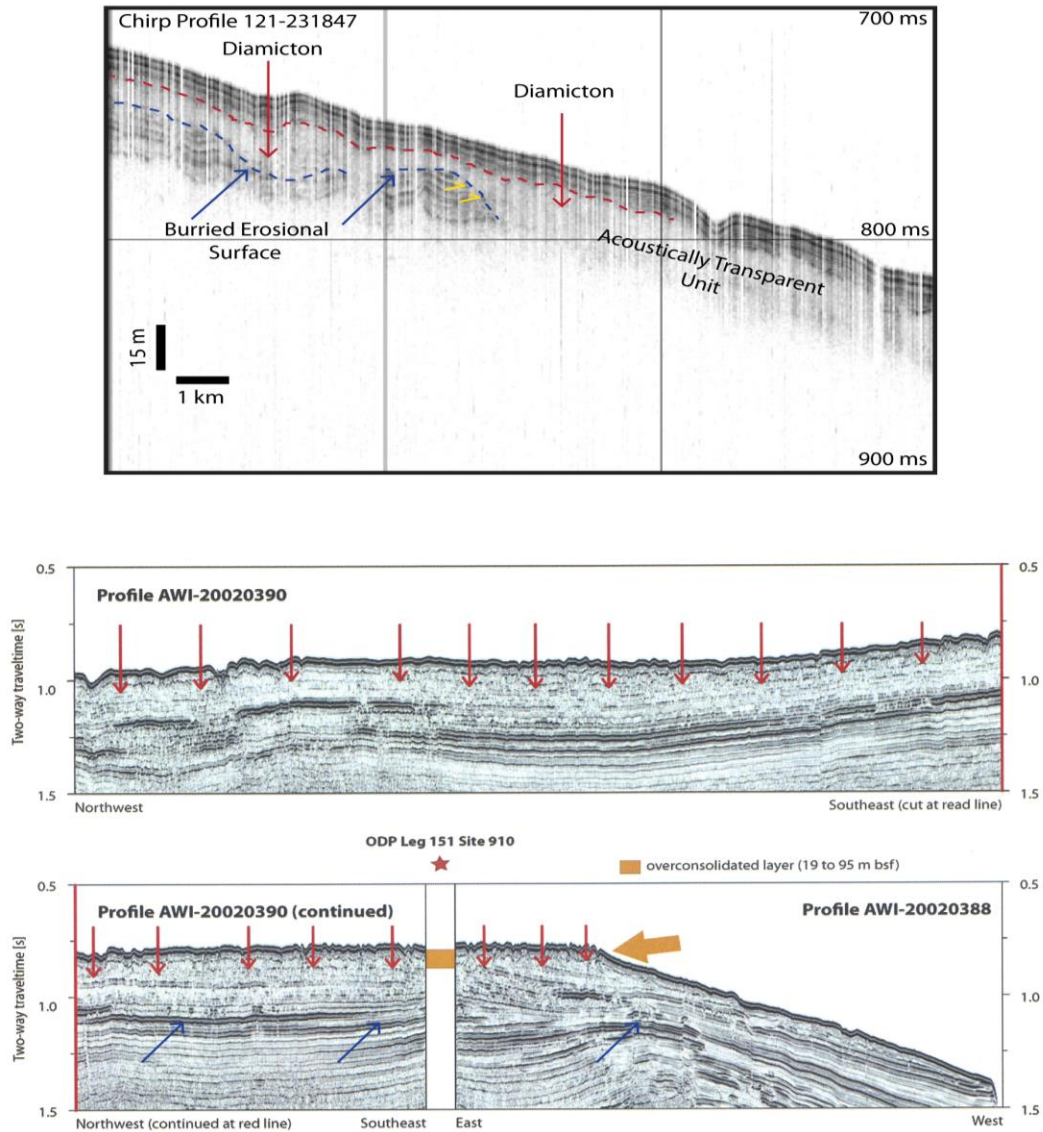


Figure 13. Correlation between Seismic reflection profile AWI-20020390 crossing ODP Site 910 (Gebhardt et al, 2011) and chirp profile 121-231847 from our study data. Tracklines of the profiles are shown in Figure 17. Red arrows point at the erosional discordance below the diamicton, and the orange arrow marks the western end of this discordance in AWI-20020390 profile. The orange box between the two seismic lines at the position of ODP Leg 151 Site 910 shows the position of the overconsolidated sediment layer in the core record. Here the similar depths for the overconsolidated section can be seen.

1. Mass wasting. Balance between gravity and the resisting forces (i.e. friction, cohesion and strength of a material) caused the slope stability. The angle of response also plays a role in whether a slope will fail or not. The missing acoustic strata (part d Figure 7) could be caused by slope failure due to steeper region or due to tectonic activity in the area. But there are several significant factors arguing against mass wasting, because there are no slide scars present in the multibeam or sub-bottom records and there are no obvious signs of mass wasting down-slope of the eroded area. Mass wasting is considered less tenable because of lack of slide scars in the interpreted acoustic records.
2. Erosion by a grounded ice sheet. This is supported by the presence of iceberg ploughmarks in the area (see Figure 7, a, b and c). This grounding event is characterized by an erosional unconformity at 20 to 30 m depth below seafloor (Figure 7) and is overlain by an acoustically chaotic layer of roughly 15 to 20 m thickness. This chaotic layer can be correlated to the diamicton described by Gebhardt et al, 2011, in the nearby area at the southern YP at about 80 ° N. This explanation is also supported by the deepest ice sheet grounding, recorded from the Arctic so far from 556 m water depth (ODP site 910, about 40 km west of the profile location) on the YP crest (Myhre et al., 1995 and Vogt et al., 1994). This grounded event has been proposed by Flower (1997) to have occurred prior to 660 ka.
3. Current controlled erosion represents the third option. The extensive erosion may have occurred during periods with different oceanographic conditions over the YP region leading to vigorous paleo-current behavior of the YP branch of WSC in the area. Acoustic profile B – B' indicated significant difference in the sedimentation pattern and acoustic layering over the southern YP region. It could be due to the presence of the YSC, which could be responsible for the lowering down the sedimentation or enhancement of the sediment erosion over the YP due to variation in the current strength.

Discussed erosional feature in profile B - B' (Figure 7) shows the unconformity on the southern YP area which indicates a major transition in glacial sedimentation from net erosion to net deposition. Flower (1997) discussed an upper regional unconformity in the western Svalbard margin and the western Barents Sea area and suggested a mid-Quaternary age for this depositional change. Howe et al. 2007 also interpreted a southward flowing bottom-current on the eastern Yermak Plateau as slope current. It could be more valuable if we try to explore this part to prove this reverse trend current by drilling in the region.

The reduced thickness patch in part e (Figure 7) could be because of low sedimentation rate due to greater transport capability of a current over the area. The acoustic layering in this thin patch are so much closed and thin that chirp signals cant not differentiate between acoustic layering and hence you cannot see any significant feature in this part rather it looks like a single thick dark acoustic layer. This is interpreted as the result of the bottom current which caused low sedimentation and high transportation rates over the 6 km patch in Figure 7.

The majority of the sub-bottom profiles acquired on the northern north eastern part of YP (Figure 6, profile C - C') display little signal penetration or possibly a homogeneous acoustically transparent to semitransparent layer with a few irregular internal acoustic reflectors at stable topographic area.

The thin patch in part 'a' of the Figure 9 (profile D - D') could also be due to low sedimentation or high transportation because of contour current activity, similar to the feature discussed in profile B - B' earlier. In Part b Figure 9 shows missing internal acoustic reflectors (80 46.520 N 12 40.295 E) at 1500 m present water depth. It could be due to low sedimentation rate and less stability at the slopes. Part c Figure 9 consists of acoustic lenses with no internal reflectors at about 2000 m present water depth. The explanation for the transparent parts in the profile D - D' is probably the redeposit sediments as described by Jakobsson et al (2013). Dowdeswell et al, (2010) also studied these kinds of features and suggested that these are the products of debris flow.

The presence of a 5 km long lighter patch in profile E - E' (part a Figure 10) could be a slumped deposit at a water depth of about 2350 m. The seismic data suggest that the deposit is not a recent structure because the deposit is covered by later sedimentation. The slumped sediments were deposited on the adjacent steep slopes from where slope failure caused the erosion to the deposit.

The 3D model in Figure 12 showing vertical curtains section, interpretation of the acoustic reflectors of the crossing profiles at the southern YP shows full 3D section. The interpreted acoustic reflectors in both profiles fits well at crossing points. Acoustic reflectors shown in the profile B - B' (Figure 7) confirms a sharp change in the acoustic thickness which probably is due to the change in sedimentation at the southern YP.

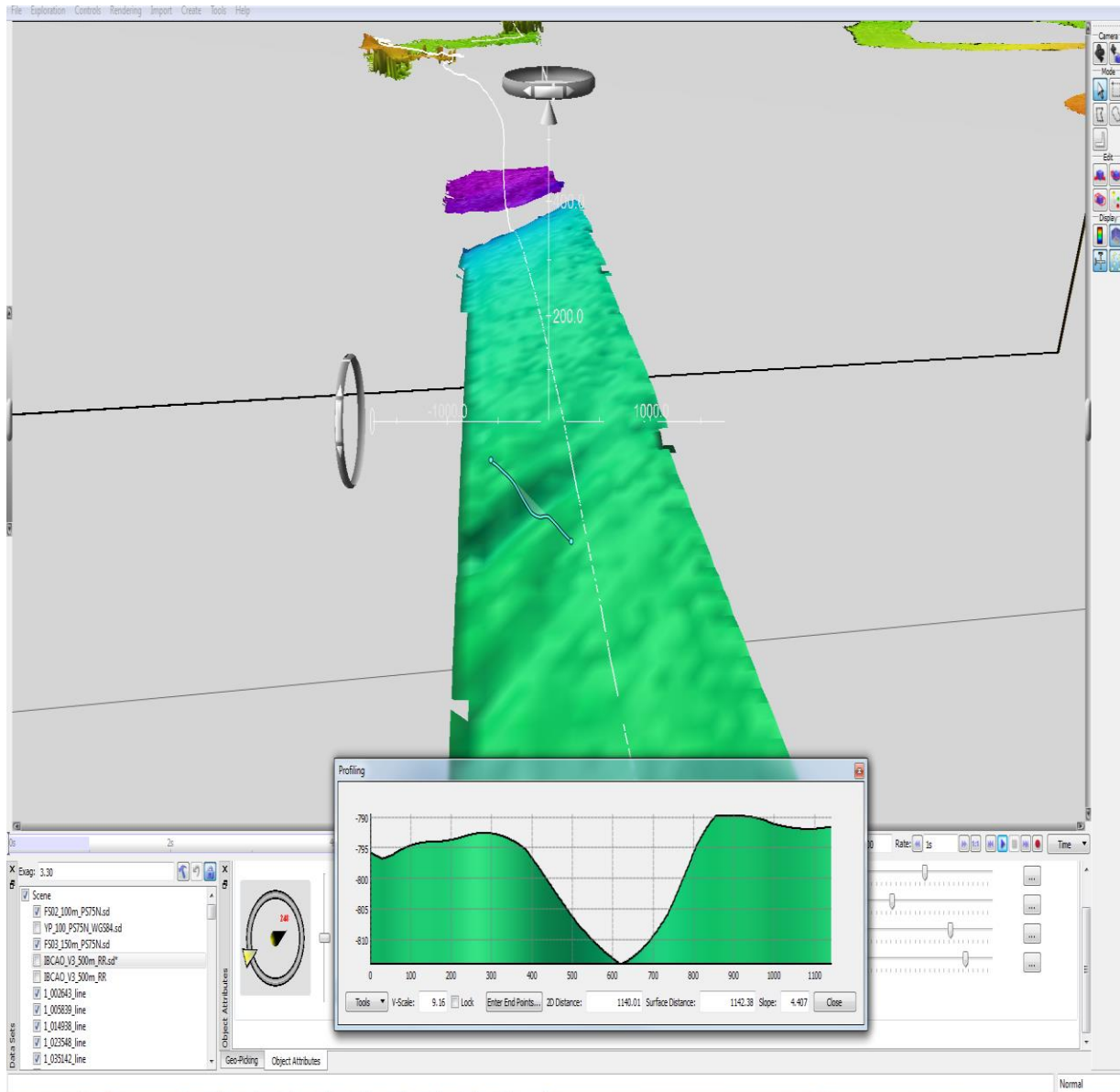


Figure 14. Profile showing deepest iceberg scar which is about 500 m wide and 25 m deep, for detail see Part c in Figure 7.

4.2 Facies Discussion

The facies F1 (Figure 11a) consists of multiple parallel to sub parallel acoustic reflectors at the southern Yermak Plateau part of the study area. This facies covers the shallow water depths up to 800 m; sediment thickness is variable and concentrated in the depressions. Similar facies have been interpreted as glaciomarine sediments, probably formed by variations in the concentration of suspended sediments (Batchelor et al. 2011). The facies F2 (Figure 11a) adjacent to facies F1 also lies at the southern YP area. But the acoustic reflectors are dark, thin and very much closed with low acoustic penetration, which could be due to some sharp change under strong force/factors. The prominent acoustic facies F3 in Figure 11a with repetitive internal reflectors indicate that the sedimentation during this time was rhythmic and thus controlled by some kind of regular forcing. This facies lies at deepest part of the study area north of YP. The appearance of this acoustic facies is recognized from previous published results and proposed to consist of glacial clay (Myhre et al., 1995). The coarser grained sediments give thicker varves with a lighter color compared to the thinner and darker winter varves mainly consisting of clay. The similar kind of facies lies at the north eastern YP (Figure 11a) also shows repetitive parallel internal acoustic reflectors under regular forcing. This facies could be also a combination of layered coarser and finer sediments. The facies F4 is found at the northern north eastern slopes of the YP. This part of the YP lies over oceanic crust and the chirp profiles show no internal reflectors (Figure 11a). Note! The varves are too thin to be resolved by chirp sonar. What you see is a residual pattern where many thin layers together make up a strong reflector.

4.3 Age Control

There is no sediment core available from this study area to correlate the acoustic facies/stratigraphy with. This means that it is not possible to verify the interpretation of the acoustic findings. The Ocean Drilling Program (ODP) leg 151 core site 911A (80.47° N and 8.23° E) and core 22JPC at (80° 29.386 N and 07° 46.141E (HOTRAX'05)) core data were considered for acoustic correlation using a synthetic seismogram, but the quality of the P-wave data was too poor to make correlation (see figure 17 for core locations). It is thus not possible to ground truth the seismic stratigraphy in the study

area because of poor seismic data (due to poor chirp data because of ice conditions during the data acquisition) and with the absence of age control due to lacking core data from the study area. It is also not possible to map facies changes for the whole study area due to bad acoustic/chirp data. North of 81° on the YP, the quality of the geophysical data is poor because of severe ice conditions (Jakobsson et al, 2010).

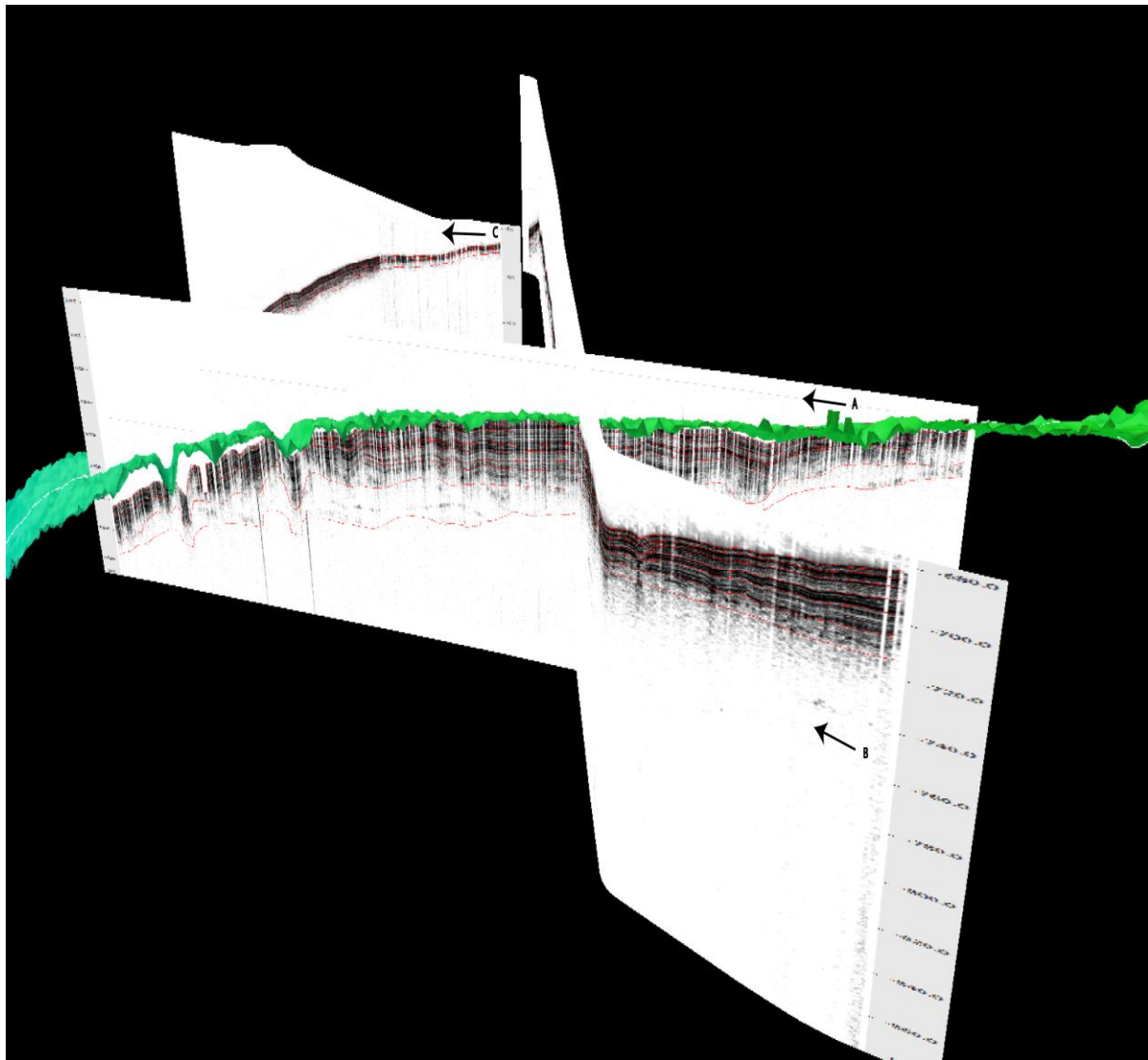


Figure 15. 3D model showing interpretation of the acoustic reflectors of the acoustic profiles at the southern YP crest. A = 102-005839, B = 818-215740 and C = 817-201252.

It should be emphasized that mismatches occur in some parts/sections between the bathymetric grids and the interpreted sea floor in explained sections (crossing curtains/profiles) see Figure 15. This is primarily the effect of two parameters: the applied flat seismic velocity of 1500 m/s for the water column and the assumption of a constant survey vessel speed. The survey speed of a research vessel is highly unlikely to remain constant during data acquisition due to varying ocean/sea conditions. However, when applying coordinates to the seismic profiles they were evenly distributed along the profiles since all were taken from the original SEG-Y data. The fact that a variable speed occurs during the surveys is therefore likely to cause the script to provide the actual shot points with slightly offset of coordinates.

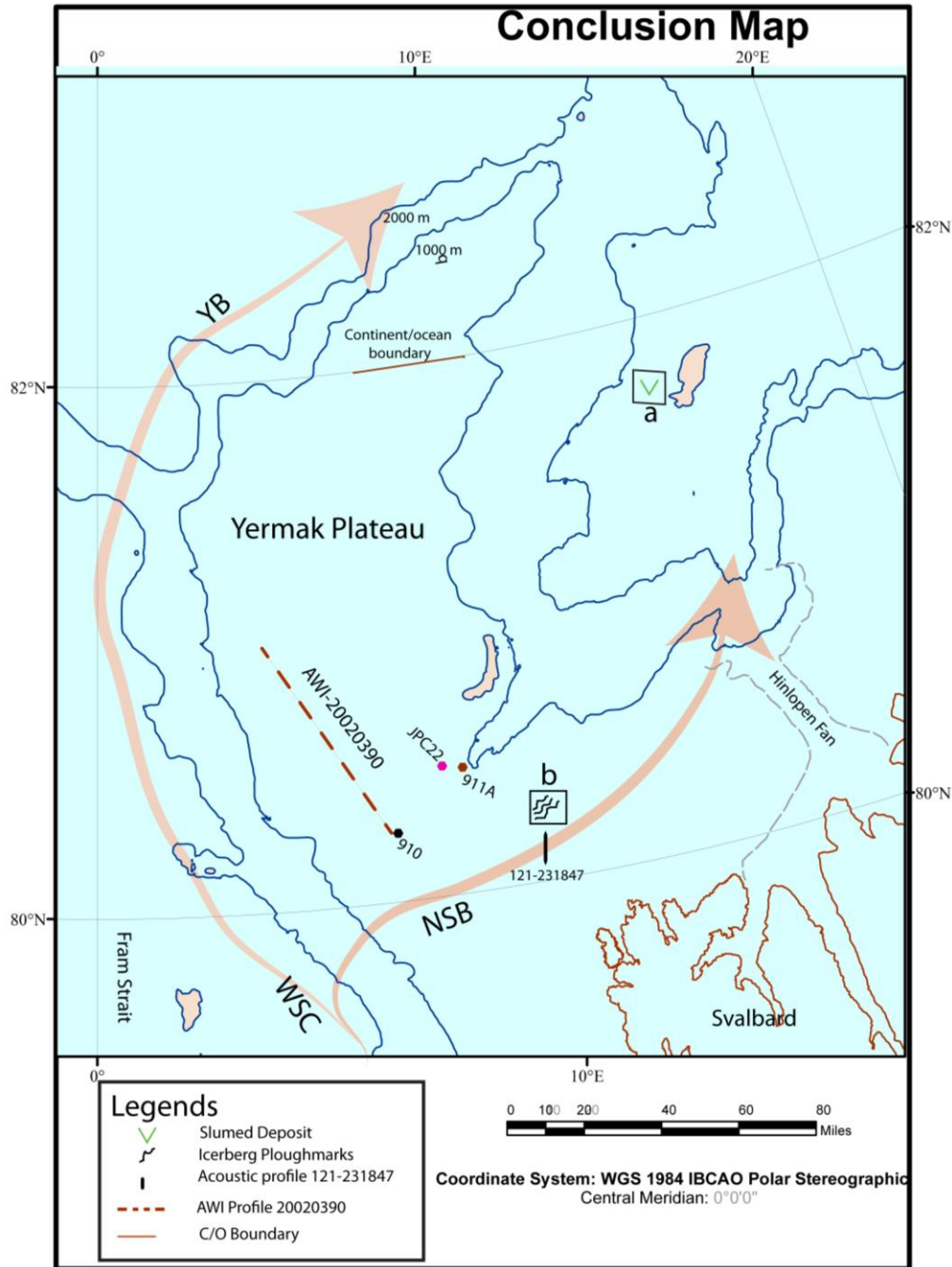


Figure 16. A compilation of all the interpreted features in this study. Red, pink and black dots show the cores location whereas black box "a" show the slumped deposit, black box "b" show the Iceberg ploughmarks location, green dot show the erosional unconformity location in this study area. Blue solid lines show the depth contours at 1000 m and 2000 m. Pink large arrows show the WSC and its branches. WSC = West Spitsbergen Current, YB = Yermak branch, NSB = Northern Svalbard branch, IPM= iceberg ploughmarks, C/O = continent ocean and AWI = Alfred Wegener Institute.

5. Conclusions

This study aims to present an overview of the seafloor morphology and shallow sedimentary structure of the YP. By analyzing 141 sub bottom profiles of 1270 km length and correlate with the multi-beam bathymetry, we try to provide an improved image of the high resolution seafloor morphology and shallow sediment structures on the YP. The major findings of this study are the following:

The data show glacial events that affected the seafloor of the YP. The deepest buried erosional unconformity depth is at 580 meter below present water depth at the southern YP. The features have been partly buried by later stage sedimentation. An ice sheet grounding event extends to 650 m present water depth characterized by an erosional unconformity at about 30 m depth below seafloor. This erosional unconformity is covered by an acoustically chaotic layer of roughly 20 m thickness, which can be interpreted as the diamicton as by Gebhardt et al, 2011, at the southern YP at about 80° N western side of this erosional unconformity. The possible explanation for the erosional event could be large scale mass wasting, grounded ice sheet on the YP crest at 550 m water depth, or current controlled erosion.

In the southernmost part of our investigated area, ploughmarks were identified at 540 – 830 m present water depth. However the problem in explaining the age for erosional events and iceberg ploughmarks observed in the study area and about the paleo-current activities remains to be answered. Deep drilled cores and core logs of the eroded area and neighboring regions might require revealing key factors including age constrains for the major events. Also a future sediment study of the area could reveal the origin of driving force/bottom current direction (see figure 16 for a detailed compilation of all study results with overview of the study area).

A detailed grain size composition/sedimentary regime history is missing in this study due to the unavailability of cores from the area. Further studies of these deposits including investigations of sediment cores may give important information about changes in paleoclimate and paleoceanographic circulation patterns through time. Due

to bad ice conditions during data acquisition, it is not possible to develop stratigraphic facies model for the entire study area.

6. References

AGAVE cruise report, 2007

Batchelor, C.L., Dowdeswell, J.A., Hogan, K.A., 2011 Late Quaternary ice flow and sediment delivery through Hinlopen Trough, Northern Svalbard margin: Submarine landforms and depositional fan. Marine Geology. Volume 284, Issues 1–4,, Pages 13–27.

Baturin, D., Fedukhina, T., Savostin, L., Yunow, A., 1994. A geophysical survey of the Spitsbergen Margin and surrounding areas. *Marine Geophysical Researches* 16: 463-484.

Cokelet, E.D., Tervalon, N., Bellingham, J.G., 2008. Hydrography of the West Spitsbergen Current, Svalbard Branch: Autumn 2001. *Journal of Geophysical Research*, VOL. 113, C01006, doi:10.1029/2007JC004150.

Dowdeswell, J.A., Jakobsson, M., Hogan, K.A., Backman, J., Evans, J., Hell, B., Löwemark, L., Marcussen, C., Noormets, R., Cofaigh, C.O., Sellen, E., Solvsten, M., 2010. High-resolution geophysical observations of the Yermak Plateau and northern Svalbard..., *Quaternary Science Reviews* doi:10.1016/j.quascirev.2010.06.002.

Engen, O., Gjengedal, J.A., Faleide, J.I., Kristoffersen, Y., Eldholm, O., 2009. Seismic stratigraphy and sediment thickness of the Nansen Basin, Arctic Ocean. *Geophys. J. Int.* 176, 805–821.

Floden, T., Bjerkeus, M., Tuuling, I., Eriksson, M., 2001. A Silurian reefal succession in the Gotland area, Baltic Sea. *GFF* volume 123, pp. 137–152.

Flower, B.P., 1997. Over consolidated section on the Yermak Plateau, Arctic Ocean: ice sheet grounding prior to 660 ka? *Geology* 25, 147e150.

Forno, G.D., and Gasperini, L., 2008. ChirCor: A new tool for generating synthetic chirp-sonar seismograms. *Computers & Geosciences* 34, 103–114.

Gebhardt, A.C., Jokat, W., Niessen, F., Matthiessen, J., Geissler, W.H., Schenke, H.W., 2011. Ice sheet grounding and iceberg ploughmarks on the northern and central Yermak Plateau revealed by geophysical data. *Quaternary Science Reviews* 30, 1726-1738.

Geissler, W.H., Jokat, W., 2004. A geophysical study of the northern Svalbard continental margin. *Geophysical Journal International* 158, 50e66.

Geissler, W.H., Jokat, W., Brekke, H., 2011. The Yermak Plateau in the Arctic Ocean in the light of reflection seismic data—implication for its tectonic and sedimentary evolution. *Geophys. J. Int.* 187, 1334–1362.

Howe, J.A. Shimmield, T.M., Harland, R., 2008. Late Quaternary contourites and glaciomarine sedimentation in the Fram Strait. *Sedimentology* 55, 179–200.

Jackson, H.R., Johnson, G.L., Sundvor, E., Myhre, A.M., 1984. The Yermak Plateau: formed at a triple junction, *J.geophys. Res.*, 89(B5), 3223-3232.

Jakobsson, M., Nilsson, J., O'Regan, M.A., Backman, J., Löwemark, L., Dowdeswell, J.A., Colleoni, F., Marcussen, C., Anderson, L, Bjork, G., Darby, D., Eriksson, B., Hanslik, D., Hell, B., Mayer, L., Polyak, L., Sellen, E., Wallin, A., 2010. An Arctic Ocean ice shelf during MIS 6 constrained by new geophysical and geological data. *Quaternary Science Reviews* 29, 3505-3517.

Jakobsson, M., Long, A., Ingolfsson, O., Kjaer, K.K., Spielhagen, R.F., 2010. New insights on Arctic Quaternary climate variability from paleo-records and numerical modeling. *Quaternary Science Reviews* 29, 3349-3358.

Jakobsson, M., Mayer, L., Coakley, B., Dowdeswell, J. A., Forbes, S., Fridman, B., Hodnesdal, H., Noormets, R., Pedersen, R., Rebesco, M., Schenke, H. W., Zarayskaya, Y., Accettella, D., Armstrong, A., Anderson, R. M., Bienhoff, P., Camerlenghi, A., Church, I., Edwards, M., Gardner, J. V., Hall, J. K., Hell, B., Hestvik, O., Kristoffersen, Y., Marcussen, C., Mohammad, R., Mosher, D., Nghiem, S. V., Pedrosa, M. T., Travaglini, P. G., and Weatherall, P., 2012, *The International*

Bathymetric Chart of the Arctic Ocean (IBCAO) Version 3.0: Geophys. Res. Lett., v. 39, no. 12, p. L12609, doi:10.1029/2012GL052219

Jakobsson et al. 2013. Arctic Ocean glacial history. Quaternary Science Reviews. **In Press**

Knies, J. & Gaina, C., 2008. Middle Miocene ice sheet expansion in the Arctic: views from the Barents Sea, *Geochem. Geophys. Geosyst.*, 9, Q02015, doi:10.1029/2007GC001824.

Kristoffersen, Y. & Husebye, E.S., 1985. Multi-channel seismic reflection measurements in the Eurasian Basin, Arctic Ocean, from U.S. ice station FRAM-IV, *Tectonophysics*, 114, 103–115.

LOMROG-II cruise report, 2009.

U.S. Congress, office of Technology Assessment, Marine minerals: Exploring Our New Ocean Frontier, OTA-O-342 (Washington, DC:U.S. Government Printing Office, July 1987).

Meridata Finland. MD 500 black-box, single/dual frequency hydrographic survey echo sounder brochure, 2008.

Milsom, John., 1989. *Field Geophysics*. Open University Press and Halsted Press in the USA, Canada and Latin America. Isbn 0-471-93248-5

Myhre, A.M., Thiede, J., Firth, J.V., et al., 1995. *Proc. ODP, Init. Repts*, 151: College Station, TX (Ocean Drilling Program). [doi:10.2973/odp.proc.ir.151.1995](https://doi.org/10.2973/odp.proc.ir.151.1995)

Parasnis, D.S., 1979. *Principles of Applied Geophysics*. 3rd edition: Halsted Press book Isbn 0-470-26480-2.

Polyak, L., and Jakobsson, M., 2011. Quaternary sedimentation in the Arctic Ocean: Recent advances and further challenges. *Oceanography* 24(3):52–64, <http://dx.doi.org/10.5670/oceanog.2011.55>.

Piechura, J., Beszczynska-Möller, A., and Osinski, R., 2001. Volume, heat and salt transport by the West Spitsbergen Current. *Polar Research* 20(2), 233–240.

Ritzmann, O., and Jokat, W., 2003. Crustal structure of northwestern Svalbard and the adjacent Yermak Plateau: evidence for Oligocene detachment tectonics and non-volcanic breakup. *Geophys. J. Int.* (2003) 152, 139–159.

Ślubowska, M.A., Koç, N., Rasmussen, T.L., Klitgaard-Kristensen, D., 2005. Changes in the flow of Atlantic water into the Arctic Ocean since the last deglaciation: Evidence from the northern Svalbard continental margin, 80_N. *Paleoceanography*, VOL. 20, PA4014, doi:10.1029/2005PA001141.

Sohn, R.A., Willis, C., Humphris, S., Shank, T., Singh, H., Edmonds, H.N., Kunz, C., Hedman, U., Helmke, E., Jakuba, M., Liljebladh, B., Linder, J., Murphy, C., Nakamura, K.-i., Sato, T., Schlindwein, V., Stranne, C., Tausenfrennd, M., Upchurch, L., Winsor, P., Jakobsson, M., Soule, A., 2008. Explosive volcanism on the ultraslow-spreading Gakkel Ridge, Arctic Ocean. *Nature* 453, 1236-1238.

Sundvor, E., and Austegard, A., 1990. The evolution of the Svalbard margins: Synthesis and new results, in *Geological History of the Polar Oceans: Arctic Versus Antarctica*, Vol. 308, of NATO ASI Series C, pp.77-94, eds Bleil, U. and Thiede, J., Kluwer Academics Publishers, Dordrecht.

Thiede, J., Myhre, A.M., Firth, J.V., and the Shipboard Scientific Party, 1995. Cenozoic Northern Hemisphere polar and subpolar ocean paleoenvironments (summary of ODP Leg 151 drilling results). *In* Myhre, A.M., Thiede, J., Firth, J.V., et al., *Proc. ODP, Init. Repts.*, 151: College Station, TX (Ocean Drilling Program), 397–420. [doi:10.2973/odp.proc.ir.151.113.1995](https://doi.org/10.2973/odp.proc.ir.151.113.1995)

Vogt, P.R., Crane, K., Sundvor, E., 1994. Deep Pleistocene iceberg ploughmarks on the Yermak Plateau: sidescan and 3.5 kHz evidence for thick calving ice fronts and a possible marine ice sheet in the Arctic Ocean. *Geology* 22, 403e406.

Matthiessen, J., Knies, J., Vogt, C., and Stein, R., 13 January 2009. Pliocene palaeoceanography of the Arctic Ocean and subarctic seas. doi:10.1098/rsta.2008.0203 Phil. Trans. R. Soc. A vol. 367 no. 1886 21-48

Lurton, X., 2002. An Introduction to Underwater Acoustics, Principles and Applications. isbn: 3-540-42967-0, Springer-Verlag Berlin Heidelberg New York.

Internet sources

Web 1. <http://doi.pangaea.de/10.1594/PANGAEA.804726>

PANGAEA database, 2013

7. Appendix

List of acoustic profiles used in this study

7.1. AGAVE 2007

| Raw data | Reference No. |
|------------------------|---------------|
| SBP 20070702002643.raw | 101-002643 |
| SBP 20070702005839.raw | 102-005839 |
| SBP 20070702014938.raw | 103-014938 |
| SBP 20070702023548.raw | 104-023548 |
| SBP 20070702035142.raw | 105-035142 |
| SBP 20070702052956.raw | 106-052956 |
| SBP 20070702090729.raw | 107-090729 |
| SBP 20070702104614.raw | 108-104614 |
| SBP 20070702112558.raw | 109-112558 |
| SBP 20070702122446.raw | 110-122446 |
| SBP 20070702132353.raw | 111-132353 |
| SBP 20070702142256.raw | 112-142256 |
| SBP 20070702152212.raw | 113-152212 |
| SBP 20070702162117.raw | 114-162117 |
| SBP 20070702172023.raw | 115-172023 |
| SBP 20070702174851.raw | 116-174851 |
| SBP 20070702174903.raw | 117-174903 |
| SBP 20070702192637.raw | 118-192637 |
| SBP 20070702210420.raw | 119-210420 |
| SBP 20070701231652.raw | 120-231652 |
| SBP 20070701231847.raw | 121-231847 |
| SBP 20070701235243.raw | 122-235243 |
| | |
| SBP 20070703012412.raw | 201-012412 |
| SBP 20070703021037.raw | 202-021037 |
| SBP 20070703034346.raw | 203-034346 |
| SBP 20070703052147.raw | 204-052147 |
| SBP 20070703061811.raw | 205-061811 |

| | |
|------------------------|-------------------|
| SBP 20070703071720.raw | 206-071720 |
| SBP 20070703081632.raw | 207-081632 |
| SBP 20070703091541.raw | 208-091541 |
| SBP 20070703101457.raw | 209-101457 |
| SBP 20070703111408.raw | 210-111408 |
| SBP 20070703121324.raw | 211-121324 |
| SBP 20070703131240.raw | 212-131240 |
| SBP 20070703141156.raw | 213-141156 |
| SBP 20070703143420.raw | 214-143420 |
| SBP 20070703161226.raw | 215-161226 |
| SBP 20070703171326.raw | 216-171326 |
| SBP 20070703181243.raw | 217-181243 |
| SBP 20070703191155.raw | 218-191155 |
| SBP 20070703194231.raw | 219-194231 |
| SBP 20070703194252.raw | 220-194252 |
| SBP 20070703202218.raw | 221-202218 |
| SBP 20070703202230.raw | 222-202230 |
| SBP 20070702220902.raw | 223-220902 |
| SBP 20070702234643.raw | 224-234643 |

7.2. LOMROG-II 2009

| | |
|------------------------|--------------------|
| SBP 20090803000211.raw | 301-000211 |
| SBP 20090803005447.raw | 302-005447 |
| SBP 20090803014725.raw | 303-014725 |
| SBP 20090803024007.raw | 304-024007 |
| SBP 20090803033243.raw | 305-033243 |
| SBP 20090803042525.raw | 306-042525 |
| SBP 20090803051802.raw | 307-0051802 |
| SBP 20090803061043.raw | 308-061043 |
| SBP 20090803070329.raw | 309-070329 |
| SBP 20090803084123.raw | 310-084123 |
| SBP 20090803093405.raw | 311-093405 |

| | |
|------------------------|-------------------|
| SBP 20090803102649.raw | 312-102649 |
| SBP 20090803114932.raw | 313-114932 |
| SBP 20090803133502.raw | 314-133502 |
| SBP 20090803152040.raw | 315-152040 |
| SBP 20090803170553.raw | 316-170553 |
| SBP 20090803185123.raw | 317-185123 |
| SBP 20090803203643.raw | 318-203643 |
| SBP 20090803222213.raw | 319-222213 |
| | |
| SBP 20090807014445.raw | 401-014445 |
| SBP 20090807032941.raw | 402-032941 |
| SBP 20090807051418.raw | 403-051418 |
| SBP 20090807065929.raw | 404-065929 |
| SBP 20090807084455.raw | 405-084455 |
| SBP 20090807103035.raw | 406-103035 |
| SBP 20090807121555.raw | 407-121555 |
| SBP 20090807140133.raw | 408-140133 |
| SBP 20090807154709.raw | 409-154709 |
| SBP 20090807173250.raw | 410-173250 |
| SBP 20090807191816.raw | 411-191816 |
| SBP 20090807210358.raw | 412-210358 |
| SBP 20090807224936.raw | 413-224936 |
| SBP 20090806235941.raw | 414-235941 |
| | |
| SBP 20090808000046.raw | 501-000046 |
| SBP 20090808012206.raw | 502-012206 |
| SBP 20090808012222.raw | 503-012222 |
| SBP 20090808030746.raw | 504-030746 |
| SBP 20090808045326.raw | 505-045326 |
| SBP 20090808063907.raw | 506-063907 |
| SBP 20090808082446.raw | 507-082446 |
| SBP 20090808101026.raw | 508-101026 |
| SBP 20090808115607.raw | 509-115607 |
| SBP 20090808134146.raw | 510-134146 |
| SBP 20090808152912.raw | 511-152912 |

| | |
|------------------------|-------------------|
| SBP 20090808171307.raw | 512-171307 |
| SBP 20090808181007.raw | 513-181007 |
| | |
| SBP 20090905001538.raw | 601-001538 |
| SBP 20090905020104.raw | 602-020104 |
| SBP 20090905034636.raw | 603-034636 |
| SBP 20090905053210.raw | 604-053210 |
| SBP 20090905071749.raw | 605-071749 |
| SBP 20090905090328.raw | 606-090328 |
| SBP 20090905104905.raw | 607-104905 |
| SBP 20090905123426.raw | 608-123426 |
| SBP 20090905141856.raw | 609-141856 |
| SBP 20090905160352.raw | 610-160352 |
| SBP 20090905174853.raw | 611-174853 |
| SBP 20090905193419.raw | 612-193419 |
| SBP 20090905211953.raw | 613-211953 |
| SBP 20090905230514.raw | 614-230514 |
| | |
| SBP 20090906002415.raw | 701-002415 |
| SBP 20090906002504.raw | 702-002504 |
| SBP 20090906021013.raw | 703-021013 |
| SBP 20090906035542.raw | 704-035542 |
| SBP 20090906054110.raw | 705-054110 |
| SBP 20090906072628.raw | 706-072628 |
| SBP 20090906091204.raw | 707-091204 |
| SBP 20090906105744.raw | 708-105744 |
| SBP 20090906124313.raw | 709-124313 |
| SBP 20090906142852.raw | 710-142852 |
| SBP 20090906161432.raw | 711-161432 |
| SBP 20090906174810.raw | 712-174810 |
| SBP 20090906174823.raw | 713-174823 |
| SBP 20090906193351.raw | 714-193351 |
| SBP 20090906211916.raw | 715-211916 |
| SBP 20090906230450.raw | 716-230450 |
| | |

| | |
|------------------------|-------------------|
| SBP 20090907004306.raw | 801-004306 |
| SBP 20090907022816.raw | 802-022816 |
| SBP 20090907041227.raw | 803-041227 |
| SBP 20090907055729.raw | 804-055729 |
| SBP 20090907065624.raw | 805-065624 |
| SBP 20090907065628.raw | 806-065628 |
| SBP 20090907074037.raw | 807-074037 |
| SBP 20090907074042.raw | 808-074042 |
| SBP 20090907075843.raw | 809-075843 |
| SBP 20090907075848.raw | 810-075848 |
| SBP 20090907094413.raw | 811-094413 |
| SBP 20090907112944.raw | 812-112944 |
| SBP 20090907131501.raw | 813-131501 |
| SBP 20090907145802.raw | 814-145802 |
| SBP 20090907164306.raw | 815-164306 |
| SBP 20090907182803.raw | 816-182803 |
| SBP 20090907201252.raw | 817-201252 |
| SBP 20090907215740.raw | 818-215740 |
| SBP 20090907234306.raw | 819-234306 |

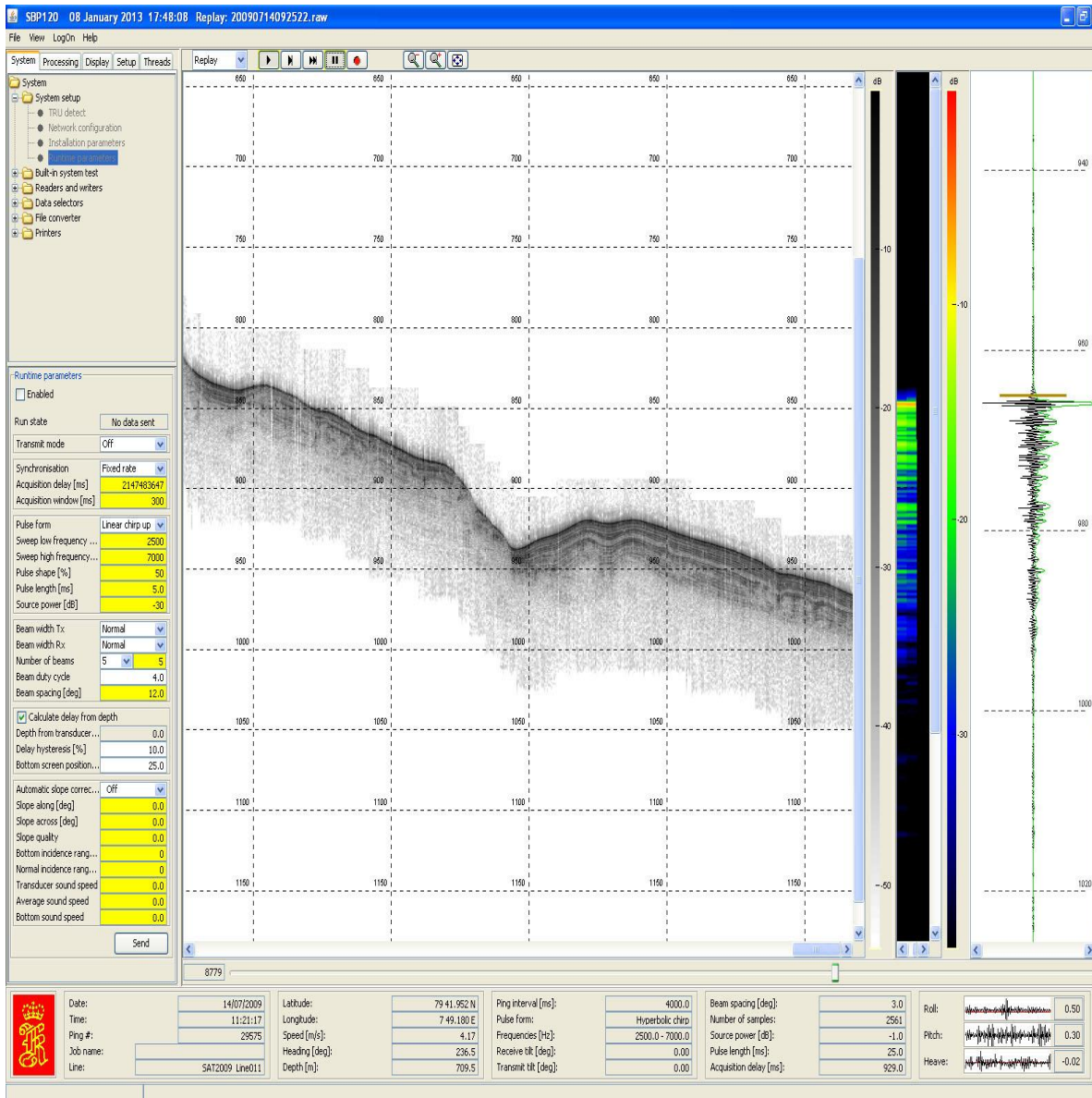


Figure A17. Screen dump of Kongsberg's SBP120 with system settings used for processing of sub-bottom profiles.

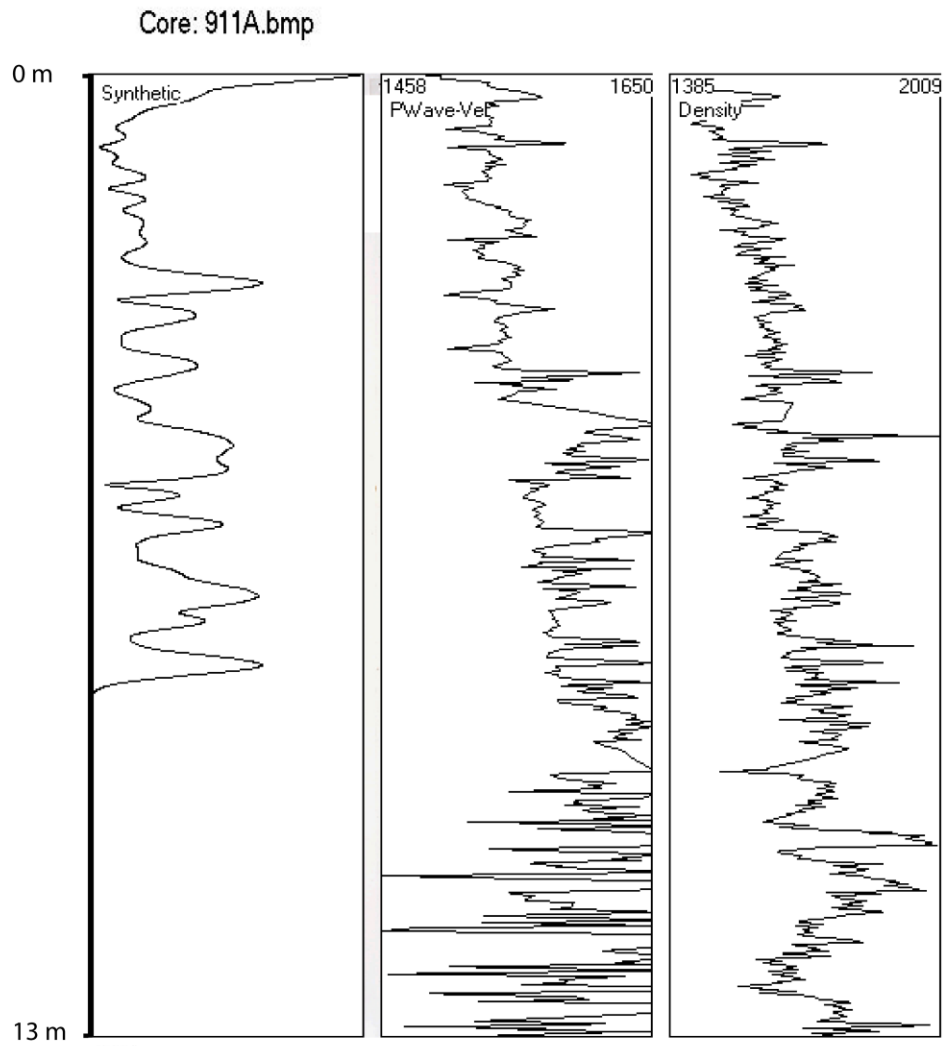


Figure A18. Output of Chircor Showing the synthetic seismogram of the ODP leg 151 core site 911A top 13 m data.

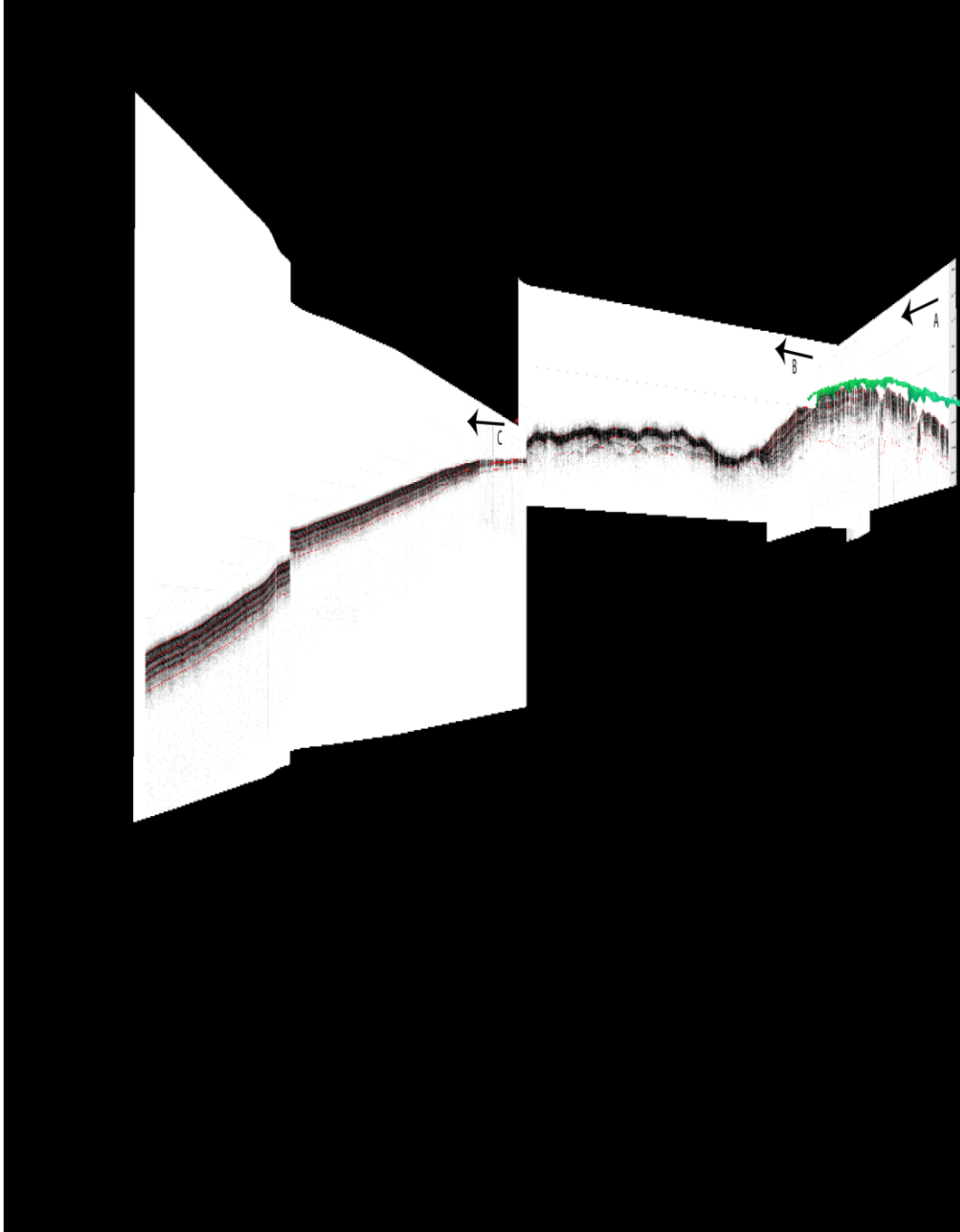


Figure A19. A 3D model showing interpretation of the acoustic reflectors of the acoustic profiles at the southern YP crest. A = 102-005839, B = 818-215740 and C = 817-201252.

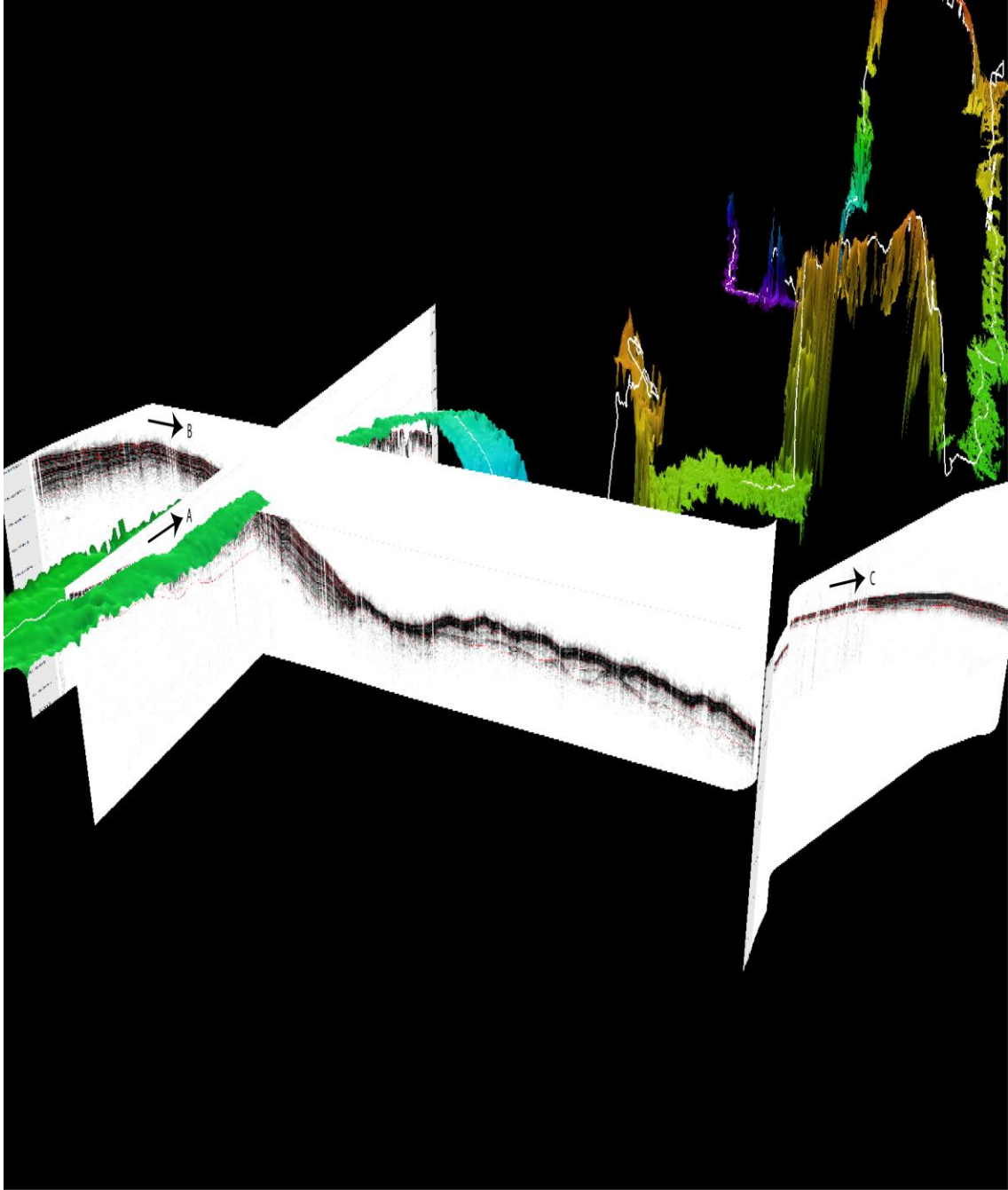


Figure A20. A 3D model showing interpretation of the acoustic reflectors of the crossing profiles at the southern YP crest. A = 102-005839, B = 818-215740 and C = 817-201252.